Cucurbit[n]urils (n = 5–8): a comprehensive solid state study

Bardelang, David; Udachin, Konstantin A.; Leek, Donald M.; Margeson, James C.; Chan, Gordon; Ratcliffe, Christopher I.; Ripmeester, John A.

Publisher's version / Version de l'éditeur:
https://doi.org/10.1021/cg201173j
Crystal Growth & Design, 11, 12, pp. 5598-5614, 2011-10-06

CRYSTAL GROWTH & DESIGN

ARTICLE

pubs.acs.org/crystal

Cucurbit[*n*]urils (*n* = 5−8): A Comprehensive Solid State Study

David Bardelang,*[,†,#] Konstantin A. Udachin,[†] Donald M. Leek,[†] James C. Margeson,[‡] Gordon Chan,[‡] Christopher I. Ratcliffe,*[,†] and John A. Ripmeester[†]

[†]NRC Steacie Institute for Molecular Sciences, 100 Sussex Drive, Ottawa, Ontario, K1A0R6, Canada

[‡]NRC Institute for Research in Construction, 1200 Montreal Road, Ottawa, Ontario K1A0R6, Canada

Supporting Information

ABSTRACT: Cucurbit[*n*]urils (CB[*n*], *n* = 5−8) have been prepared, separated, and purified, and the structure of their solid state assemblies has been addressed. A number of general features were identified which are of interest to understand some peculiar properties of cucurbiturils (solubility, aggregation, assembly, transformation to porous crystals, influence of air humidity). CB[5], CB[6], and CB[8] were isolated as hydrate crystals whose structures were found to show a strong tendency of the macrocycles to interpenetrate. A self-closing effect was rationalized in terms of multiple weak CH···O interactions between the macrocycles, the degree of which is discussed in detail. Solid state cross polarization magic angle spinning (CP-MAS) ^{13}C NMR spectra obtained at 900 MHz were correlated with the crystal structures. An odd−even effect in the crystallinity of thermally treated CB samples (CB[5] and CB[7] amorphous, CB[6] and CB[8] crystalline) was observed, which is reflected in differences in water solubility (CB[5] and CB[7] are water-soluble, whereas CB[6] and CB[8] are only very scarcely so). This may be explained by a less efficient self-association for CB[5] and CB[7] as compared with CB[6] and CB[8], which is reflected in the number of inter-cucurbituril CH···O interactions per cucurbituril. This leads to a more favorable solvation for the CBs having an odd symmetry, whereas those with even symmetry prefer to self-associate in a manner ultimately leading to crystallization. We also propose an explanation for the presence of anions (Cl^-) inside some cucurbituril materials, whose cavity is often considered hydrophobic. Furthermore, it is demonstrated that large quantities of the very stable microporous CB[6] crystals (which have the $R\bar{3}$ channel structure) can be obtained very easily by a simple thermal treatment of the hexagonal crystals of CB[6] (*P6*/*mmm* structure) obtained directly from the initial reaction used to synthesize the various CB[*n*]. The micromorphology of the CB[*n*] powders was established using scanning electron microscopy (SEM), and the tendency of each material to absorb water from the atmosphere was demonstrated by thermogravimetric analyses (TGA).

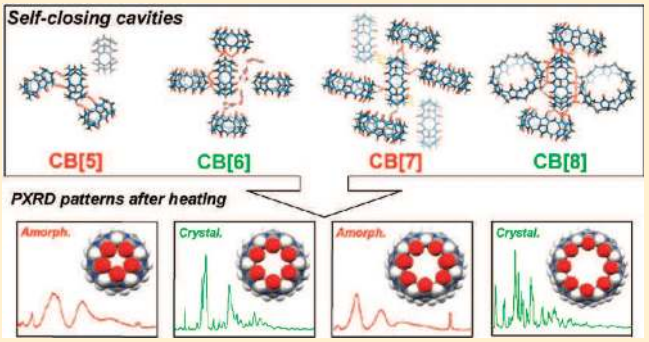

INTRODUCTION

Cucurbit[*n*]urils (CB[*n*]) are glycoluril-based macrocycles possessing a constricted hydrophobic cavity delineated by two identical, polar carbonyl fringe portals (Chart 1).[1,2] They are attracting more and more interest because of their unprecedented properties, as for example their extremely strong binding toward ferrocene derivatives (reaching a value comparable with that of the avidin·biotin pair),[3] their potential for the construction of novel topologies[4] and molecular machines,[5] peptide recognition[6] and their use as drug carriers,[7] to cite a few examples. Efforts are still ongoing to fully understand their formation mechanism, and a comprehensive study on that point has been published recently.[8] However, a detailed characterization of the solid materials obtained after the synthesis and purification of CB[*n*] has not been reported.[9]

Some of us recently reported that electron spin resonance (ESR) spectroscopy could be used to observe the initial step of the aggregation process of CB[7] and CB[8] in water[10] with the aid of a small paramagnetic probe that is included in the self-assembling macrocycles.[11] We have also shown in previous papers that cucurbiturils crystallize in certain cases to form water-filled channels either through a columnar arrangement of CB[6] or CB[8] (where water molecules are confined by the inner surface of the cucurbiturils)[12] or by the cyclic hexamer stacking of CB[5] in HCl hydrate crystals (where water molecules are in the space defined by the center of the hexamer, that is, by the outer surface of the cucurbiturils).[13] Kim and coworkers recently showed that CB[6] could self-assemble in certain conditions to yield porous organic crystals that can absorb acetylene efficiently.[14] There are one-dimensional (1D) channels in these crystals which are defined by the outer surface of the CB[6] in a manner reminiscent of the hexamer crystal of CB[5]. The CB[6] crystals proved to be extremely stable upon heating, considering that it is a crystal made from macrocycles held

Received: September 7, 2011
Revised: October 4, 2011
Published: October 06, 2011

Chart 1. Molecular Structure of Synthetic Host Molecules CB[5] to CB[8][a]

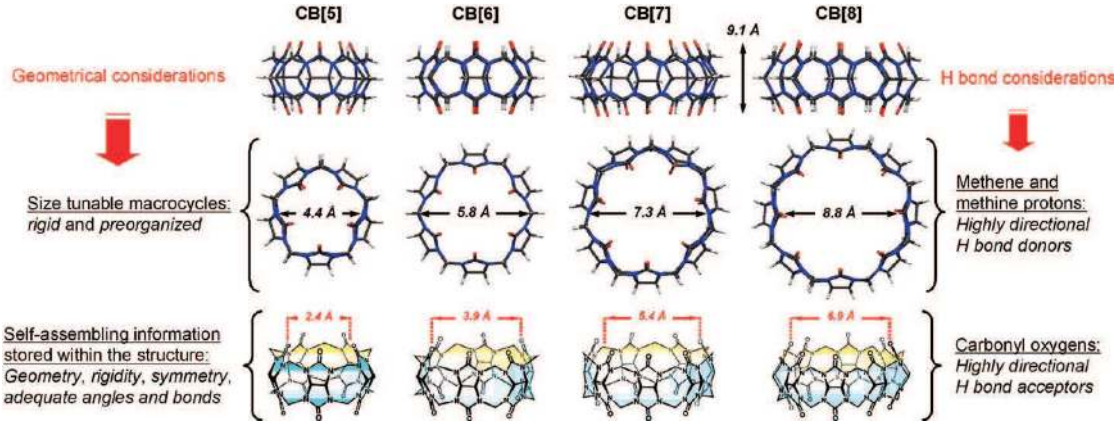

[a]Internal van der Waals free diameters are indicated at the widest and narrowest sections.

together by weak CH···O interactions.[15] A possible explanation may lie in the number of these hydrogen bonds.[16] The CH···O interactions thus appear to be a very powerful factor in defining crystal assembly for the whole family of cucurbiturils. However, a comprehensive description of the phases obtained after purification for each cucurbituril (crystallinity, strength of the assembly, water content, micromorphology) and a quantitative description of the hydrogen bond schemes present in the CB[*n*] crystals have not been presented in the literature to the best of our knowledge. Therefore, it appeared that a general *solid state* study of the cucurbiturils was needed, which could provide a comprehensive view of the phases obtained after the purification steps and thus facilitate the use of the most important CB[*n*]s for supramolecular[17] applications starting from well-characterized solid powders. In this paper, we describe the isolation of eight representative phases based on CB[5] to CB[8] and the characterization of these materials by a combination of several solid state techniques.

EXPERIMENTAL SECTION

Preparation and Purification of CB[*n*], *n* = 5, 6, 7, 8. *General procedure:* typically, glycoluril (100 g, 0.704 mol) was added to a 500 mL round-bottomed flask equipped with a magnetic stir bar. A 37% HCl solution (142 mL) was then added to the flask. Paraformaldehyde (42.2 g, 1.407 mol) was slowly added, allowing the solution to stir well. The viscous solution was allowed to stir for 30 min more until the solution set as a gel, which then was heated to 100 °C resulting in a rapid dissolution of the gel. This solution was refluxed for 17.5 h at 100 °C, then allowed to cool to room temperature, and the stirring was stopped in order to allow the formation and growth of crystals during the next 24 h. The synthesis yields a mixture of CB[5], CB[6], CB[7], and CB[8] as the main macrocycles, but *i*CB[6],[2k] *i*CB[7],[2k] and CB[5]@CB[10][5b] were also present as impurities. The purification of the cucurbiturils depends on several parameters.[2c,d] One can rely on solubility differences between the macrocycles (followed by recrystallization when possible) or proceed through successive recrystallization in a time-consuming procedure. In the course of our solid state study of cucurbiturils, we found a somewhat easier procedure to get the whole set of macrocycles (from CB[5] to CB[8]) by combining the procedures proposed in the seminal papers of Kim[2c] and Day.[2d] For the Kim paper,[2c] the synthesis is similar but the purification is quite different principally relying on fractional dissolution/crystallization/precipitation with water/acetone mixtures (except for CB[8]). The proposed method of this work is somewhat closer to that reported by Day et al.,[2d] which allows for rapidly obtaining large quantities of fractions highly enriched in the desired cucurbituril as well as pure fractions in our case (especially for CB[6] and CB[8]). Using aqueous HCl 37% as the reaction solvent, the solution was left to stand for one day after reaction, after which high purity hexagonal crystals of CB[6] with the perfect stack structure previously reported (CB[6]·2HCl·36H_2O)[12] were obtained. Another important observation was that upon heating in an oven to 100 °C for 48 h these crystals transformed into a *polycrystalline* powder whose powder X-ray diffraction (PXRD) pattern (see Figure 10) corresponded to the channel *porous* structure first determined by Kim et al.[14] This method allows large quantities of *polycrystalline porous* CB[6] to be produced very easily (up to 17 g for the best batch) for gas sorption measurements and other applications.

Purification of CB[8]. The solution remaining after the CB[6] crystals were collected was evaporated, yielding a sticky-yellow solid. 88 mL of a formic acid solution prepared with 90 mL of HCOOH (90%) and 110 mL of distilled water was added to this dark-yellow solid with vigorous stirring. As the material was digested a white suspension formed. Another 70 mL of the formic acid solution was added to help dissolve the remaining yellow solid. The mixture was stirred for 1 h in order to solubilize as much material as possible, and the suspension, consisting of pure CB[8], was collected by suction filtration. Note that CB[8] is still somewhat soluble in this mixture, and one should use as little acid solution as possible. On the other hand, not adding enough formic acid may result in partial purification with small amounts of CB[6] present. This filtered material was found to have the same basic structure (PXRD measurements) as the material obtained after recrystallization: CB[8] can be quickly recrystallized reproducibly and very easily from a concentrated hot aqueous 37% HCl solution to give **CB[8]C**. It was also possible to wait for the first crystals to appear at around 80 °C before cooling to room temperature. We also found that CB[8] could be dissolved in a large amount of hot water, and the amorphous-looking material obtained after filtration and rapid removal of the water under reduced pressure using a Rotavap was labeled **CB[8]A**. Finally, it was found that the CB[8] materials obtained by these methods were isostructural (crystalline, space group $I4_1/a$, Figure S2, Supporting Information) with each CB[8] almost perpendicular to one another (perhaps the most representative of the "general case")[18] and not perfectly aligned as has been found for samples grown from nitric acid.[12] In fact, the self-penetration for CB[8] macrocycles seems so powerful (in the absence of any competing interactions) that it can drive the assembly of CB[8] host−guest complexes (in these cases the guest

dx.doi.org/10.1021/cg201173j |*Cryst. Growth Des.* 2011, 11, 5598–5614

molecules do not protrude from the cavity) into isostructural single crystals[7m] or organic nanosheets[19] in which self-closing is the essence of the assembly. **CB[8]C**: ^{1}H NMR δ 4.28 (d, 2H, J = 15.2 Hz, CH_2), 5.60 (s, 2H, CH), 5.89 (d, 2H, J = 15.2 Hz, CH_2).[2c] CB[8], 4 HCl, 15.1 H_2O (single crystal XRD).

Purification of CB[6]. The filtrate obtained after removal of the CB[8] suspension, containing CB[5], CB[6], and CB[7], was then evaporated to dryness and redigested using water, in which CB[6] is very sparingly soluble. 400 mL of distilled water was added before stirring overnight. The new suspension was filtered using a glass frit covered by a small filtration paper to prevent the CB[6] from clogging the pores of the frit. The white powder must be washed several times with water in order to purify it, but even after up to *12* washes with 75 mL of distilled water, the powder still contained about 10% of CB[7] as assessed by ^{1}H NMR. However, the use of ultrasound greatly helped in the purification process:[20] after the 400 mL solution had been filtered once, the white powder was collected and placed in a 250 mL Erlenmeyer flask together with about 150 mL of distilled water. The flask was put in a heated ultrasound bath (~55 °C), and after 30 min a thick *foam*-like suspension had formed. The suspension was then filtered under a vacuum, and this step was repeated one more time resulting in a good purity CB[6] sample, labeled as **CB[6]A**. We fortuitously discovered that CB[6] can be recrystallized either (i) from a dilute sulphuric acid solution of CB[6] (200 mL with about 4 g of CB[6] afforded ~0.4 g of **CB[6]CC** after 3 months) or (ii) by allowing acetone to diffuse into a dilute aqueous hydrochloric acid solution over a one month period (1 L flask with about 5 g of CB[6] in 200 mL of dilute HCl gave 1.5 g of **CB[6]C** collected as acid free fine white needles containing: CB[6], water, and acetone; see structure **2** below).[21] **CB[6]CC**: ^{1}H NMR δ 4.31 (d, 2H, J = 15.6 Hz, CH_2), 5.59 (s, 2H, CH), 5.83 (d, 2H, J = 15.6 Hz, CH_2).[2c] CB[6], 4.66 H_2O (single crystal XRD).

Purification of CB[7]. The filtrate resulting from the purification of CB[6] now contained CB[5] and CB[7], which were separated as follows. The solution was reduced to 100 mL volume under reduced pressure followed by the addition of ~750 mL of methanol and stirring overnight. After the stirring was stopped, a precipitate of CB[7] slowly deposited at the bottom of the flask, which was then filtered on paper and washed several times with ~20 mL of methanol. The product was then put in an oven at 70 °C for 1 day to remove the methanol. This procedure generally produced pure CB[7] as an amorphous white material that has a tendency (if not dried right after the filtration and washing steps) to adsorb water, giving a very viscous yellow liquid. If CB[6] was still present, CB[7] was dissolved again in distilled water, put in an ultrasound bath, and refiltered to remove the CB[6] and get the pure product (**CB[7]A**). The pH was also observed to increase as a function of the washing steps (with *ultrasound*) presumably as a result of the gradual removal of acid (i.e., HCl involved in earlier steps).[20] All attempts to recrystallize the CB[7] were unsuccessful. Indeed, there are only a very few known crystal structures of CB[7].[2c,22] This difficulty in obtaining crystalline forms may be due to CB[7]'s tendency to structure itself in aqueous acid solutions and thus form supramolecular gels.[22] **CB[7]A**: ^{1}H NMR δ 4.30 (d, 2H, J = 15.6 Hz, CH_2), 5.60 (s, 2H, CH), 5.86 (d, 2H, J = 15.6 Hz, CH_2).[2c] CB[7], 3.2 HCl, 5.6 H_2O (elemental analysis).

Purification of CB[5]. The filtrate resulting from the CB[7] isolation was put on a rotavap until 100 mL of the methanol was left. To this was added 800 mL of acetone. This was allowed to stir for several hours before filtration on filter paper and collection of a white crystalline powder. We then recrystallized the product using aqueous HCl solutions (9 mL of 37% HCl for 3 g of crude CB[5]). This purification was particularly successful and reproducible in the cases where CB[5] was the major species. The solution was heated to dissolve the CB and allowed to cool down and evaporate in order to form crystals, **CB[5]C**. The same procedure as for **CB[8]A** was used to try to prepare amorphous samples of CB[5], that is, dissolution in water followed by quick solvent removal under reduced pressure and vigorous stirring to produce **CB[5]A**. **CB[5]C**: ^{1}H NMR δ 4.43 (d, 2H, J = 15.6 Hz, CH_2), 5.65 (s, 2H, CH), 5.81 (d, 2H, J = 15.6 Hz, CH_2).[2c] CB[5], 3.75 HCl, 10.88 H_2O (single crystal XRD).

It should be stressed that the composition and purity of the materials obtained are sensitive to the experimental conditions (temperature, time of reaction, acid concentration), and in this regard we relied very much on ^{1}H solution NMR to follow the progress at each purification step. In summary: (a) In most cases we isolated up to several grams of crystals of each CB[n] using concentrated HCl or H_2SO_4 solutions, which, with the exception of CB[7], seem to produce CB[n] crystals of assignable structure and composition quite reliably (samples **CB[5]C**, **CB[6]C**, **CB[6]CC**, and **CB[8]C**). (b) Since CB[7] was always obtained as an amorphous powder, we also tried to produce amorphous materials of the other CB[n] both for comparison with **CB[7]A**, and with the crystalline forms (samples **CB[5]A**, **CB[6]A**, **CB[7]A**, and **CB[8]A**).

Single Crystal X-ray Crystallography. Single crystal X-ray diffraction data were measured on a Bruker Apex 2 Kappa diffractometer at 100 K, using graphite monochromatized Mo Kα radiation (λ = 0.71073 Å). The unit cell was determined from randomly selected reflections obtained using the Bruker Apex2 automatic search, center, index, and least-squares routines. Integration was carried out using the program SAINT, and an absorption correction was performed using SADABS.[23] The crystal structures were solved by direct methods, and the structure was refined by full-matrix least-squares routines using the SHELXTL program suite.[24] All atoms were refined anisotropically. Hydrogen atoms on cucurbituril molecules were placed in calculated positions and allowed to ride on the parent atoms.

Liquid State NMR. All the solution NMR spectra were recorded using a Bruker DRX-400 spectrometer, operating at 400.13 MHz for ^{1}H and 100.62 MHz for ^{13}C. 2D spectra were recorded using an inverse-detected gradient probe. ^{13}C Spectra were recorded using a directed-detected broadband probe. Standard Bruker pulse sequences were used for all experiments. Some proton and carbon spectra were recorded on a Bruker AV-III 400 spectrometer operating at 400.13 MHz for ^{1}H and 100.62 MHz for ^{13}C using a Bruker BBFO probe. All spectra were recorded in the following solvent mixture: $D_2O/CF_3CO_2D/D_2SO_4$ (1/1/0.15) and referenced to the methine protons of the CBs.[2c]

900 MHz CP-MAS ^{13}C NMR Spectroscopy. Solid state cross-polarization magic angle spinning (CP-MAS) ^{13}C NMR spectra were obtained at 226.36 MHz (21.1 T, 900 MHz for ^{1}H) on the Bruker Avance II 900 spectrometer of the National Ultrahigh Field NMR Facility for Solids (Ottawa, Canada), using double resonance Bruker 4 mm and 3.2 mm MAS probes spinning at 6 and 14 kHz, respectively. A cross-polarization time of 4 ms was used with recycle times of 4−8 s. Chemical shifts were referenced to TMS using adamantane as secondary reference.

Thermogravimetric Analysis (TGA). TGA results were acquired on a TA 2050 analyzer under nitrogen flows of 40 and 20 mL·min^{-1}. TGA curves were first measured with a heating ramp of 5 °C min^{-1} from room temperature to 500 °C.

Powder X-ray Diffraction. Diffractograms were recorded on a Bruker D8 Advance diffractometer using Cu Kα radiation at λ = 1.54053 Å. Reflections were collected from 5 to 60° in 2-theta with steps of 0.03° and a step time of 189 ms at 17 °C.

Scanning Electron Microscopy. Micron scale images were acquired on a Hitachi S-4800 cold field emission scanning electron microscope (SEM), fitted with two secondary detectors. Images were acquired using a mixed image of the two signals at a working distance of 8 mm, at a beam energy of 2 keV and a current of 5 μA. The dry samples were deposited onto aluminum stubs on adhesive carbon tapes, and regions of interest were imaged at several magnifications to show the grain size and micromorphology.

Table 1. Summary of Single Crystal X-ray Diffraction Results

crystal structure	1	2	3	4
trivial name	CB[5]C	CB[6]C	CB[6]CC	CB[8]C
composition	CB[5], 3.75 HCl, 10.88 H_2O	CB[6], 1 acetone, 8 H_2O	CB[6], 4.66 H_2O	CB[8], 4 HCl, 15.1 H_2O
T/°C	−100	−173	−173	−173
crystal system	orthorhombic	orthorhombic	trigonal	tetragonal
space group	*Pbam*	$Cmc2_1$	$R\bar{3}$	$I4_1/a$
a, Å	28.709(1)	19.574(1)	32.036(9)	28.108(4)
b, Å	17.337(1)	15.805(1)	32.036(9)	28.108(4)
c, Å	19.464(1)	15.840(9)	12.417(7)	21.896(7)
α, °	90	90	90	90
β, °	90	90	90	90
γ, °	90	90	120	90
V, Å^3	9687.6(3)	4900.4(5)	11036.7(8)	17299.2(7)
Z	8	4	9	8
final R_1	0.085	0.066	0.130	0.127
peak/hole, e A^3	+2.27/−2.43	+0.71/−0.39	+1.52/−0.52	+1.38/−0.49

RESULTS AND DISCUSSION

As a consequence of our preliminary findings, we focused our attention on aqueous HCl prepared cucurbituril materials (with the exception of **CB[6]CC**). Our objective was to prepare a sufficiently broad and representative panel of CB based materials to study (i) their crystalline state, (ii) their aggregation behavior, (iii) structural changes under thermal treatment (whose purpose was to evacuate remaining solvent to get pure materials), and (iv) the uptake of water by the desolvated materials.

Single Crystal X-ray Diffraction. The tendency of cucurbiturils to *self-penetrate* by means of weak CH···O interactions between the outer ring protons of one CB (methene and methine protons) and the ureido carbonyl oxygens of a neighbor in a perpendicular fashion has been noted previously.[14,22,25] A fully self-included complex would be physically impossible due to the rigid and constricted glycoluril core. This occurs via CH···O close contacts that are usually expected to be only weakly involved in the overall framework stability. Indeed, when other forces are active in solution during the crystal growth, for instance, when cations are present and hence ion-dipole interactions are possible, the carbonyl rims are observed to coordinate the cations thereby precluding any significant CH···O interactions.[26] Nevertheless, CH···O hydrogen bonds can be very powerful, especially in the case of cucurbiturils, where their numbers per macrocycle can be sufficient to ensure the crystal an impressive thermal stability.[14] Hydrochloride hydrate crystals were obtained for CB[5] and CB[8] (structures **1** and **4**), whereas acetone hydrate and pure hydrate crystals were isolated for CB[6] (structures **2** and **3**, respectively). The main structural data are summarized in Table 1.

The use of salt free aqueous acid solutions to purify the cucurbiturils by recrystallization avoided closure of the CB cavity by coordinated cations (which can also be a strong drawback for recognition studies).

Structure **1**, **CB[5]C**, shown in Figure 1, crystallized in the *Pbam* space group and displays a quasi-symmetrical cavity which contains a chloride anion and is capped with two water molecules (Figure 1a). There are two CB[5]@Cl^- complexes in the asymmetric unit, and the chloride anions are not positioned exactly at the center of the cavity. At first sight, it seems odd that the cavity of CB[5], that is supposed to be hydrophobic, has an anion inside. However, close inspection reveals that the anion is always closer to ureido carbons (mean distances 3.58 and 3.93 Å for the first CB[5] in the asymmetric unit, 3.71 and 3.80 Å for the second) than to the nitrogens (3.86 and 4.05 Å for the first CB[5] and 3.92 and 3.97 Å for the second). In fact, the CB[5] scaffold is constructed such that it forms an electropositive microenvironment due to 10 slightly electropositive carbons in the cavity (the ureido carbons are all connected to three electron-withdrawing atoms, one oxygen and two nitrogens). The hydrogen atoms involved in the water network of hydrogen bonds (vide infra) were also located. Interestingly, there are close contacts between bridging methylene hydrogens and C═O oxygens on neighboring CB[5] units (two H···O distances of 2.79 and two of 2.46 Å) arranged in 1D zigzag chains running in opposite directions along axis *b* and closing the CB[5] cavities on one side (Figure 1b). We found two kinds of CB[5] planes in which the opposite 1D chains are of a different symmetry; see Figure 1c where in the yellow colored CB[5] planes, the chains stack in register along dimension *a*, whereas in the blue colored CB[5] planes there is an offset of ∼4 Å along axis *b*. The two different planes stack alternately along the *c*-axis, defining constricted channels (green circle of Figure 1b running along axis *c*) that are connected to the perpendicular zigzag channels in the *ab* planes (space between the CB chains) where water, chloride ions, and acid protons form a dense hydrogen bonded network, which also interacts with the CBs by additional hydrogen bonds. This structure is different from the one reported in 2000 (synthesis of CB[6] homologues[2c] showing a dense packing of CB[5]). The present **CB[5]C** structure also exhibits channels different from those reported by us[13] and others[27] for crystals grown under similar conditions.

Single crystals of CB[6] of suitable quality for X-ray studies were first obtained as a water and acetone solvate and are interesting because of the *absence* of any metal cations and any anions, which are often used to obtain single crystals of cucurbiturils.[9,25,26] Structure **2**, **CB[6]C**, shown in Figure 2, was solved in the $Cmc2_1$ space group and shows a composition of one CB[6] for one acetone and eight water molecules. Another crystal structure free of any salt and acid for CB[6] has been reported recently[28] (water and diethyl ether solvate). The two

dx.doi.org/10.1021/cg201173j |*Cryst. Growth Des.* 2011, 11, 5598–5614

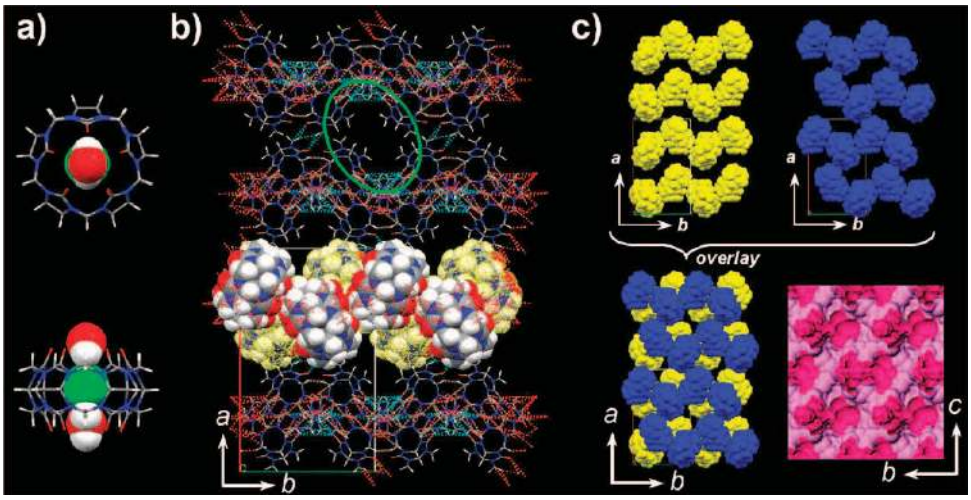

Figure 1. Structure **1**, **CB[5]C**. (a) The CB[5] cavity contains a chloride anion and is capped with two water molecules. (b) The CB[5] are engaged in multiple inter CB[5] CH···O interactions principally forming 1D zigzag chains running in opposite directions along axis *b*. The water and chloride zigzag chains of the [110] planes are connected by the small channels along *c* (green circle) via a dense network of H bonds (not shown for clarity). (c) The CB[5] zigzag chains, separated by water and chloride anions, form alternate layers in the [110] planes. They stack along crystallographic axis *c* so that the CB chains face each other in a non-interacting manner (successive yellow and blue colored CB planes, see the overlay depicting a 2 × 2 × 1 array of unit cells). In the bottom right-hand corner of (c) a slice of the *bc* plane perpendicular to the *a*-axis illustrates the space accessible to a sphere of diameter 1.0 Å running in the network defined by the CB[5] arrangement (i.e., where the water and chloride would be located). In this view from above, dark pink shows the outside surface of the void spaces which are completely inside the box, whereas light pink shows the inside surface of those void spaces which are sliced by the top face of the box. For clarity, the guest and solvent are not shown in (b) and (c).

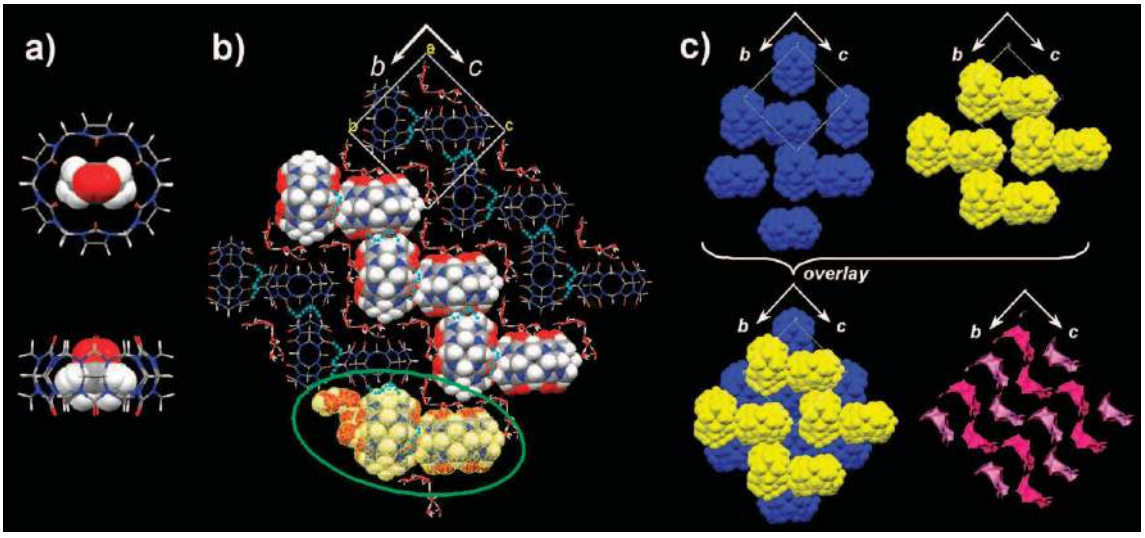

Figure 2. Structure **2**, **CB[6]C**. (a) Disordered acetone is included inside CB[6]. (b) CB[6] are disposed perpendicular to one another so that the macrocycle cavity is partially closed on one side only. The other side of each macrocycle is hydrogen bonded with water clusters (green circle) forming 1D zigzag chains alternating with CB[6] chains within the [011] planes in a manner reminiscent of superimposed stairs. (c) Expansion of this recognition motif clearly shows the half self-closure of the cavities for CB[6] that are arranged in alternate layers with an offset of the [011] planes of ≈8.4 Å along direction *b*. The three-dimensional packing illustrates the successive layers (blue and yellow) along the *a*-axis for the construction of a 1 × 2 × 2 array of unit cells. Corrugated 1D tubes (c, bottom right) depicting the space available for water, complementary to the CB[6] network. In this view from above, dark pink shows the outside surface of the void spaces which are completely inside the box, whereas light pink shows the inside surface of those void spaces which are sliced by the top face of the box. The guests are omitted for clarity in (b) and (c).

crystals are isostructural and differ only in the guests included in the CB[6] cavity and their slightly different unit cell parameters.

The acetone molecule is found to be entirely included inside each CB[6] unit, disordered over two positions inside the distorted cavity (O···O distances between oppositely positioned oxygen atoms of one rim are in the 6.73−7.33 Å range) and does not participate in additional interactions in the crystal (Figure 2a). However, we note a very strong $CH_{(ac.)}\cdots C_{(CB[6])}$ contact between an acetone hydrogen and a ureido carbon of CB[6] with a distance of 2.42 Å (well below the sum of van der Waals radii of 2.90 Å) and an H···C═O angle of 95.5°. The acetone hydrogen is thus positioned almost perpendicular to the

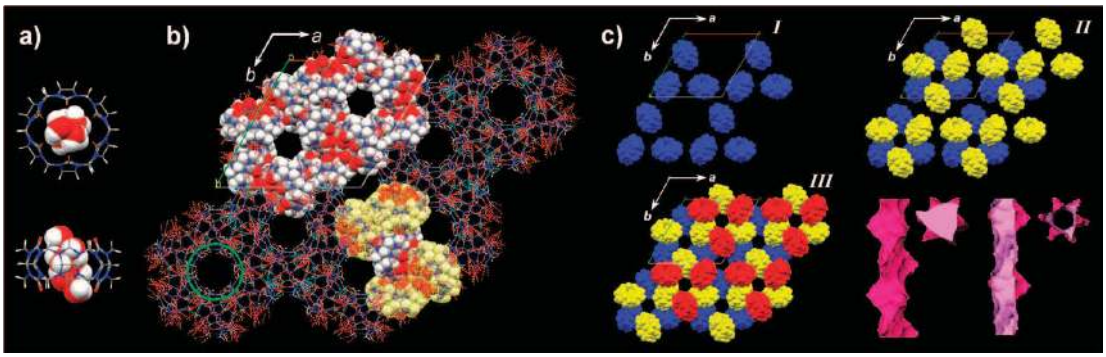

Figure 3. Structure **3**, **CB[6]CC**. (a) Inclusion of ordered water in CB[6]. (b) The CBs are now completely self-closed by their nearest neighbors by means of multiple CH···O interactions (see the four macrocycles highlighted in yellow) and form a honeycomb-like hexagonal framework with water filled channels (green circle). (c) The three-dimensional packing, illustrating the successive layers (*I*, *II*, *III*) along the *c*-axis for the construction of a $2 \times 2 \times 1$ array of unit cells, and the structure of the vertical channels aligned with the *c*-axis (viewed from above, dark pink shows the outside surface of the void spaces which are completely inside the box, whereas light pink shows the inside surface of those void spaces which are sliced by the top face of the box). The guests were removed for clarity in (b) and (c).

carbonyl carbon atom that is quite reminiscent of the possible role of these carbons in stabilizing the chloride anions in the CB[5] cavities of structure **1**.[29] The CB[6] macrocycles of structure **2** are found to be engaged in CH···O hydrogen bonds principally via the outside ring hydrogen atoms: the carbonyl oxygens on one rim are found to interact strongly with water, while three oxygens of the other rim interact with CHs from another CB[6] disposed perpendicularly. Thus, the two cucurbituril rims are not symmetry related when considering the surrounding molecules (see the alternating zigzag chains of water and CBs in Figure 2b). The [011] planes composed of the alternate chains of water and CB[6]@acetone are not packed in register, Figure 2c, but there is an offset of approximately 8.4 Å along direction *b*.[30]

We later found that, similar to Kim's CB[6] structure, which has thermally stable channels,[14] sulphuric acid can be used with water to crystallize CB[6] in an identical way. Indeed, CB[6] was found to crystallize slowly in the $R\bar{3}$ space group showing the same water channels (Figure 3) from a mixture of CB[5], CB[6], and CB[7] and a water/H_2SO_4 mixture (250/30 mL). Structure **3**, **CB[6]CC**, shown in Figure 3, has six ordered water molecules included inside CB[6] and two among these six molecules hydrogen bond to each rim of the cucurbituril (Figure 3a).

These two molecules belong to the plane defined by the ureido carbonyl oxygens of each rim and hydrogen bond to two of the carbonyl oxygens leaving the four remaining carbonyls free for the self-closing motif to take place. Interestingly, all the oxygen atoms of the water molecules point inward in the cavities meaning that they direct their hydrogens toward the macrocycles walls. Two of them form modestly close contacts with ureido nitrogens (O−H···N: 2.66 Å, 172.4°) and the remaining two form stronger interactions with carbonyl carbons (O−H···C: 2.44 Å, 172.6°). The CB[6] are arranged in such a way as to effect *self-closing* of their cavities (Figure 3b) but without intermediate water, in contrast with structure **2** (the cavity self-closing seems here the highest possible with each rim directly surrounded by one neighboring macrocycle). The degree of multiple weak CH···O interactions engaged between each cucurbituril might reach a level sufficient to account for the surprising stability of the entire supramolecular framework (see Powder X-ray Diffraction (PXRD) section and Figures 6 and 7).[14] Consider for example the four highlighted CB[6] in yellow (Figure 3b); two of them (back and front) give hydrogen bonds toward the CB[6] in the middle, whereas the two others receive C−H contributions from the central one. Each cucurbituril participates in two cyclic hexamers. Indeed, Figure 3c shows (section II) four hexamers resembling six-pointed stars composed of three yellow and three blue CBs (as part of a $2 \times 2 \times 1$ array of unit cells). But when we add a new CB layer on top of it (the red ones), we see that all yellow colored CBs are part of a new hexamer. This particular arrangement gives rise to channels with 6-fold symmetry, with hydrophobic surfaces defined by the methene and methine protons of CB[6] (Figure 3c, bottom right). The channel space is then filled with water molecules.

CB[7] proved to be very difficult to crystallize. Indeed, very few crystals with CB[7] are known, including the structure reported by Kim et al.,[22] which again shows *self-closure* of the cucurbituril cavities, and the first-reported CB[7] structure which is self-penetrated to a lesser extent.[2c]

CB[8] crystals were obtained easily from hot or cold 37% aqueous HCl solutions. Structure **4**, **CB[8]C,** shown in Figure 4, was found to belong to the $I4_1/a$ space group with a composition of one CB[8] for 4 HCl and 15 water molecules.

This structure is therefore isostructural with the original one reported by Kim in 2000[2c] except that two sulphates have been replaced by four chloride anions and the water content is slightly different. The CB[8] cavity is entirely filled with disordered water molecules, the chloride anions being located outside (Figure 4a). As for structure **3**, we note the presence of three moderately close contacts (H···C=O_1: 2.66 Å, 65.1°; H···C=O_2: 2.59 Å, 94.7°; H···C=O_3: 2.53 Å, 51.4°) and one with the atoms positioned much closer (H···C=O_4: 2.36 Å, 82.6°). Despite a slightly higher *R* factor than the one reported before, we found all hydrogens in structure **4** allowing a precise description of the role of H-bonds in this structure. Again the CH···O close contacts are found to play a critical role with 9 inter-cucurbituril H bonds per carbonyl rim spread among 3−5 carbonyl oxygens, whereas the others are stabilized by classical water mediated H-bonds. Each cavity is once again partially *self-closed* (Figure 4b) in a motif reminiscent of that found in all other aqueous acid grown crystals (structures **1**, **2**, and **3**). Finally, the CB[8] stack (Figure 4c) so that they form a 3D connected network of channels (Figure 4d) in which water and chlorine are found to interact with the macrocycles.

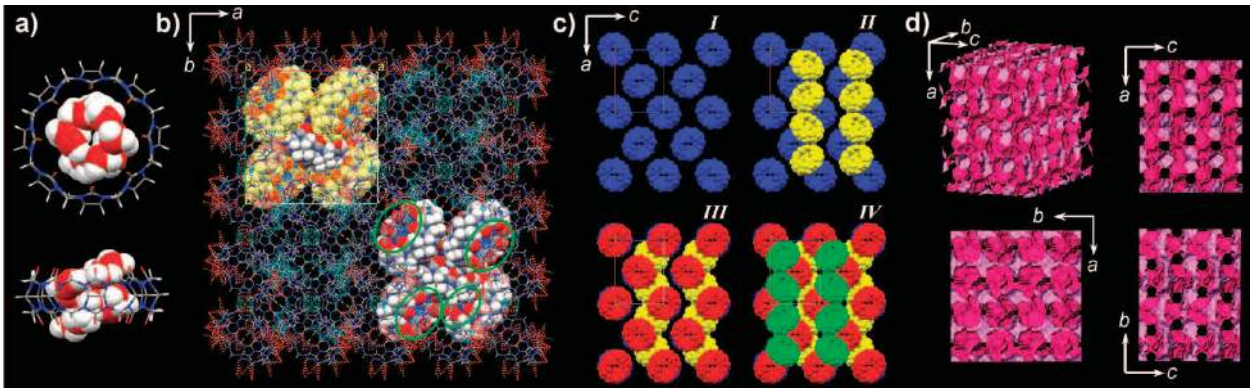

Figure 4. Structure **4**, **CB[8]C.** (a) Inclusion of disordered water in CB[8]. (b) As for structure **3**, we clearly see the importance of CH···O interactions by a similar self-closing of each macrocycle (green circles in b) by two closest neighbors (see the four highlighted CB[8] in yellow, two of which give hydrogen bonds whereas the two others receive contributions from the central one). (c) The three-dimensional packing, illustrates the successive layers (*I*, *II*, *III*, *IV*) along the *b*-axis for the construction of a 2 × 1 × 2 array of unit cells. (d) The structure of the 3D connected network of channels, depicting the space available for water and chlorine, featuring a 2 × 2 × 2 array of unit cells. In this view from above, dark pink shows the outside surface of the void spaces which are completely inside the box, whereas light pink shows the inside surface of those void spaces which are sliced by the top face of the box. The guests are omitted for clarity in (b), (c), and (d).

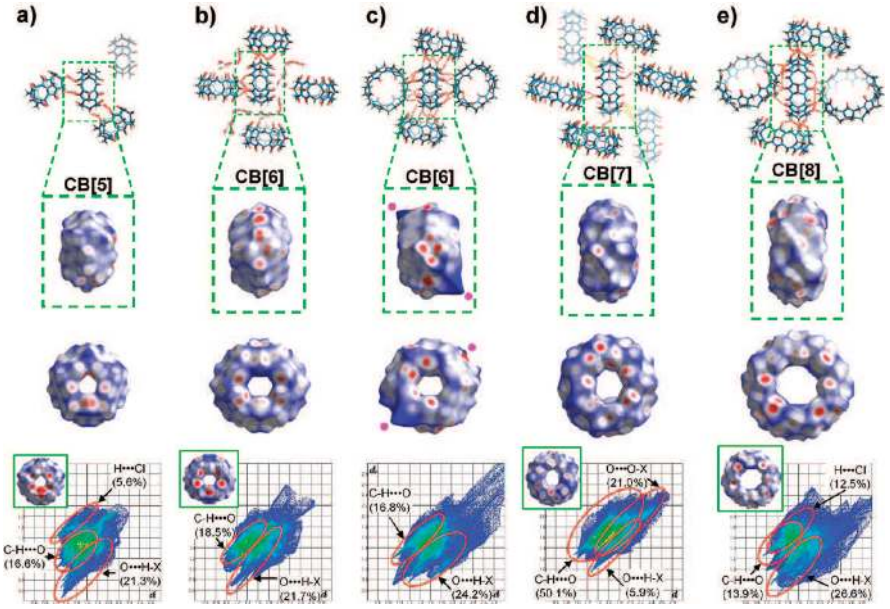

Figure 5. Highlight of the *self-closing* motif found in all cucurbituril crystals in which the CBs are not engaged in other competitive interactions such as ion complexation: (a) CB[5] in structure **1**; (b) CB[6] in structure **2**; (c) CB[6] in structure **3**; (d) CB[7] from the literature;[22] (e) CB[8] in structure **4**.[35] All cucurbiturils have most of their hydrogens which behave as donors engaged in multiple weak CH···O interactions with neighboring macrocycles and their carbonyl oxygens as acceptors toward surrounding CB methene and methine protons {water, HCl, H_2SO_4, and acetone have been omitted for clarity except in (b) and CB−CB CH···O hydrogen bonds highlighted in the immediate surroundings of the central cucurbituril}. Hirshfeld surfaces (d_{norm}) are also displayed as side and top views accounting for all intermolecular interactions regarding the central molecule. The corresponding fingerprint plots (bottom line) are also shown, to further support this self-assembling motif and separate the OH···O from the CH···O contributions. Insets show the Hirshfeld surface of the opposite side of the CBs except in (c) for which the surface is identical. The red, white, and blue areas account for inner surface atoms being at a distance respectively shorter, approximately equal, and longer than the sum of van der Waals radii when considering the corresponding nearest atoms of the surrounding molecules. The blue spikes on the CB[6] surfaces (c, pink dots) are from the absence of molecules in this area as a consequence of not assignable electron densities.

Thus, the cucurbituril skeletons appear to be highly rigid and predisposed to establish specific intermolecular interactions.

Indeed, it seems that the self-assembling information is *stored* within the structure[15−17,31] as the CB geometry, rigidity, and symmetry and accordingly adequate angles and bonds mean that it is almost inevitable that methene and methine protons will engage in multiple weak H bonds with carbonyl oxygens. To get an overview of all intermolecular interactions surrounding the cucurbiturils in the crystals, we used the Hirshfeld surface analysis introduced by Spackman and co-workers[32] mapped with parameter d_{norm}[33] using the software *CrystalExplorer*[34] for all crystals of the present study, and the one reported by Kim for CB[7] in 2007[22] (Figure 5).

dx.doi.org/10.1021/cg201173j |*Cryst. Growth Des.* 2011, 11, 5598–5614

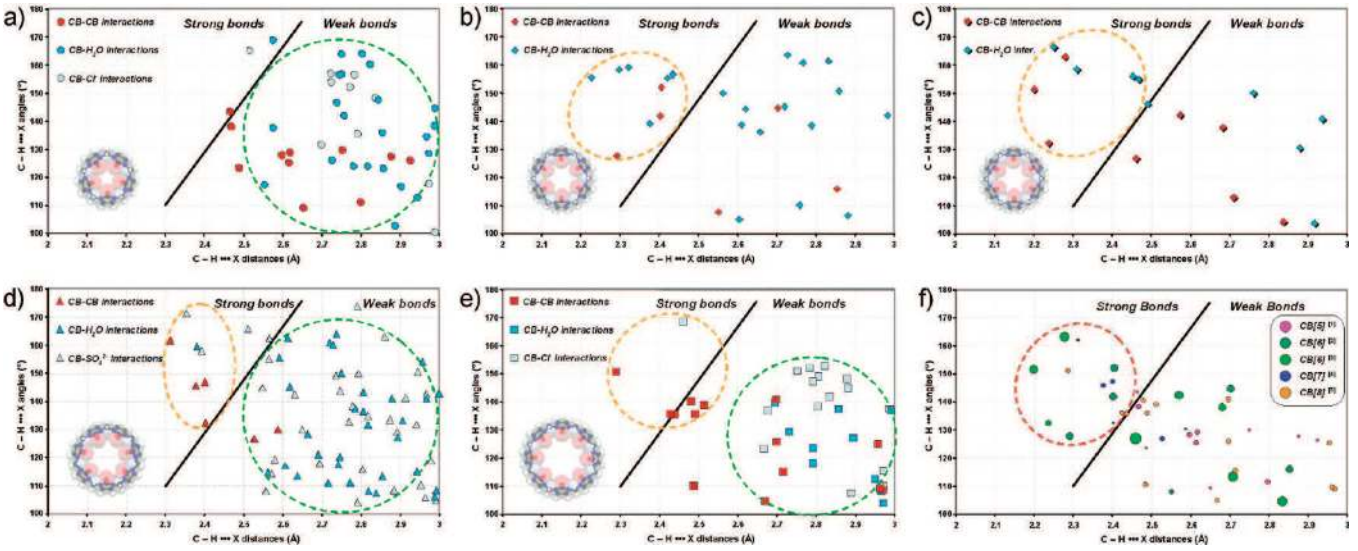

Figure 6. Plot of the occurrence and strength of C−H···O and C−H···Cl^- interactions in crystal structures of (a) CB[5] in structure **1** (circles), (b) CB[6] in structure **2** (diamonds), (c) CB[6] in structure **3** (shadowed diamonds), (d) CB[7] from the literature[22] (triangles), (e) CB[8] in structure **4** (squares), and (f) an overview of the CB−CB C−H···O interactions per unit cell as a function of the macrocycles averaged to an identical number of CBs per cell. Each hit accounts for intermolecular distances below 3.0 Å and angles above 100° for C−H···X interactions involving all cucurbiturils in the unit cell of the crystals considered.

The aim of this approach was to provide a picture of all close contacts and to decipher each possible contribution thereby enabling one to view the molecule as a *whole* in the context of its intermolecular interactions.[36] This method of imaging and quantifying the extent of each contribution was motivated by getting insights into the self-assembling features of cucurbiturils in the solid state where competitive forces are also present (i.e., water and acid molecules solvating the macrocycles and hampering *self-closing* of the cavities). However, as powerful as this approach can be, the crystal structure under study needs to be well-characterized, as emphasized by Spackman et al.[32] Cucurbituril crystal structures are generally difficult to solve and especially to refine as they often contain many water molecules and show extensive disordering, which constitute severe drawbacks, rendering their crystal structure determination quite challenging. Given these concerns, we worked on the precise identification of the solvent molecules and cocrystallized guests and modeled their disorder.[37]

The most remarkable feature of CB[*n*] assemblies, which appears to be general in the solid state, is the *cross* organization (Figure 5 top line) which maximizes the interactions between the external methene/methine protons of one CB with the carbonyl crown oxygens of another CB (Figure 5 second and third lines). This behavior is unusual considering the strength of OH···O hydrogen bonds (expected to be ubiquitous in our case) with respect to significantly weaker CH···O interactions. Indeed, one might expect the carbonyl oxygens to be preferentially engaged in OH···O hydrogen bonds as all the crystals contain water and some of them HCl or H_2SO_4, thus precluding the formation of the *self-recognition* motif. On the contrary, the weak CH···O interactions seem to be driving the crystal assemblies of all cucurbiturils so as to maximize their numbers and their cumulative strength, presumably as a consequence of the very rigid and preorganized geometry of the macrocycles that have a high content of directional bonds. This is consistent with the idea of *self-association* of growing oligomers during the synthesis of cucurbiturils[8] as suggested by Isaacs and co-workers and is also quite reminiscent of the concept of multivalency[6h,38] (several carbonyl oxygens can host multiple H bonds per cucurbituril rim). This proves to be rather decisive when the Hirshfeld surfaces are considered, whose red dots point to a high number of interactions per cucurbituril, especially for CB[6] (Figure 5b,c) and CB[8] (Figure 5e and see also Figure 5 top line for comparison). Indeed, we found that CB[5] (Figure 5a) and CB[7] (Figure 5d) are significantly less associated with their nearest neighbors as compared with CB[6] and CB[8] that form a dense network of interactions with surrounding molecules. However, OH···O hydrogen bonds certainly play a crucial role in stabilizing the overall framework as pictured in Figure 5 (bottom line) in the fingerprint plot analyses[39] (see also insets of Figure 5a,b in which intense red dots denote stronger OH···O interactions). These interactions compare favorably to CH···O interactions. Nevertheless, the fraction of the CH···O close contacts is sufficient for the *cross* scaffold to be present in all the structures studied (except that of CB[5], Figure 5a). Also note the high fraction of CH···O interactions for CB[7] (Figure 5d bottom, 50.1%) with respect to the amount of OH···X interactions (only 5.9% of the overall amount of intermolecular interactions). This can be ascribed to the high content of sulfate anions whose oxygens are highly hydrogen bonded by virtue of the CB outside protons. Also, the extent of OH···X interactions might be underestimated owing to the absence of hydrogens (presumably not located) in the solvent molecules of the CB[7] crystal structure, thus resulting in a strong deviation from the actual values.[37] The great merit of Hirshfeld surfaces (and also of the properties that can be mapped on them) is that they give a clear depiction of intermolecular interactions acting in the space surrounding the cucurbiturils, in inherently complex solvate molecular crystals. However, in order to better understand the occurrence of the *cross* arrangement of the macrocycles, we focused

dx.doi.org/10.1021/cg201173j |*Cryst. Growth Des.* 2011, 11, 5598–5614

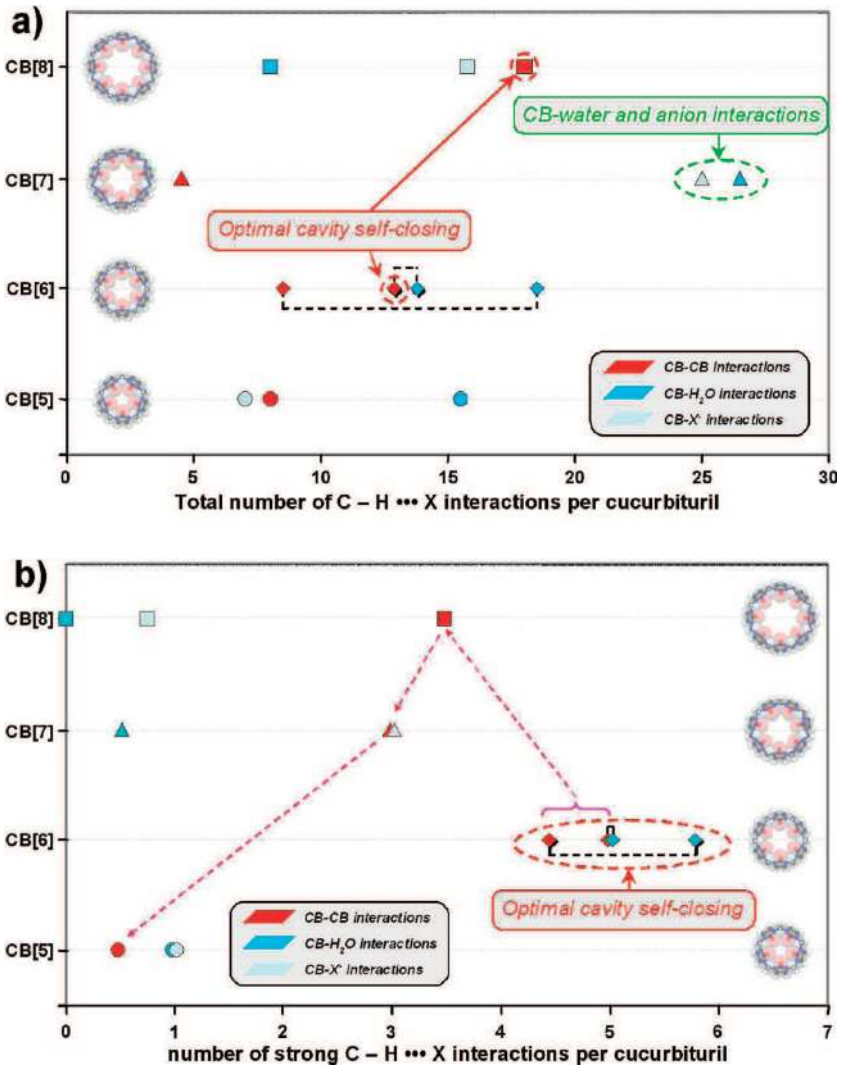

Figure 7. (a) Total number of C−H···X interactions per cucurbituril, and (b) number of *strong* C−H···X interactions per cucurbituril, highlighting the stability of CB[6] and CB[8] crystals. The symbols are identical to those used in Figure 6. The pink dashed arrows are to suggest an order of structural stability for the intercucurbituril network in the crystal structures.

on CH···O and CH···Cl^- interactions and assessed their number as well as their strength by a careful examination of the crystal structures (Figure 6).

We also separated the CB(CH)−water(OH_2) contributions (as pictured in sky blue) from the CB(CH)−CB(O═C) interactions (as pictured in red). CB−water interactions account for the vast majority of hits appearing in the *weak bonds* section. CB(CH)−Cl^- (CB[5] and CB[8]) and CB(CH)−O^- (CB[7]) interactions are displayed in light blue and play an important role for the CB[5] and CB[7] crystals (Figure 6, panels a and d, respectively). In this representation, we chose to highlight CH···X^- (X═Cl or O) interactions of the hydrogen bond type (directional interaction, the CH···X^- angle should roughly range between 130 and 180° for a distance below 3.0 Å) and ignore the weaker CH···X^- ion−dipole interactions (CH···X^- angle near 90°).[40] For CB[5] and CB[7], it seems that the possible CB−CB interactions are diluted within the solvent and acid molecules, precluding the formation of an intense network of cucurbiturils maintained by CB−CB interactions (this can also be related to the greater solubility of these two CBs in water). This can also explain the relative thermal fragility of the crystals (see PXRD section below). However, one should consider the interactions appearing at a distance below the sum of van der Waals radii, that is, for an H···Cl distance ≤ 2.95 Å and an H···O distance ≤2.72 Å.[41] In this regard, CB[5] and CB[7] are the cucurbiturils that show the highest number of *strong* CH···X^- interactions (the oblique line in Figure 6 should be slightly shifted to higher intermolecular distances for CH···Cl^- interactions) that may explain the "glue" behavior already reported for CB[7] gels formed in acidic aqueous solutions.[22] As suggested by Hay and co-workers, the presence of two electron-withdrawing atoms (each carbon is connected to two nitrogen atoms throughout the rings) *increases* the acidic character of the C−H protons thus strengthening the corresponding H bonds.[40,42] Protonation of carbonyl groups at very low pH has also been reported to induce CB[6] and CB[7] aggregation, an additional feature to explain the "glue" behavior.[10b] Conversely, the two CB[6] crystals show a relatively low number of "competitive" interactions (in the sense of loosening the overall CB−CB framework), especially in the case of structure

3 (Figure 6c) for which the vast majority of hits (considering their total number; see Figure 6f) comes from CB−CB interactions. Also note the occurrence of three particularly strong bonds (intermolecular distance below 2.3 Å). These unique features may account for the exceptional stability of this crystal structure (as for the cucurbituril framework) maintained by CH···O interactions (see PXRD section and ref 14). CB[6] structure **2** shows a more significant contact with water molecules for the cucurbiturils as evidenced by the higher number of competitive H bonds in the overall diagram (also highlighted in the *strong bonds* section; see also Figures 2b and 5b). CB[8] (Figure 6e) represents an intermediate case (between the situations encountered for CB[5], CB[7], and CB[6]) for which a significant number of CB−CB interactions are positioned in the center (*moderate bonds*) region and competitive CB−water and CB−Cl^- interactions in the *weak bonds* section (albeit to a lesser extent as compared with the number of hits for CB[5] and CB[7]). Finally, Figure 6f compares the CB−CB C−H···O interactions per unit cell as a function of the macrocycles, normalized to the same number of cucurbiturils (big and small dots are for high and low numbers of interactions respectively). Again, the two CB[6] structures have the strongest and the highest number of intercucurbituril interactions (CB[6] structure **3** is the one presenting the most robust *self-closing* network). The corresponding interactions for CB[5] are spread in the *weak bonds* section, whereas those of CB[7] are in the *strong bonds* section, but this does not account for the huge number of competitive interactions also found in this last case (see Figure 6d the dashed green circle). These results may explain why CB[5] and CB[7] evolve to *amorphous* phases after drying while CB[6] and CB[8] retain some degree of *crystallinity* and also the surprising thermal stability of CB[6] structure **3** well above 100 °C (see PXRD section).

To further assess the importance of intercucurbituril interactions in the physical properties of the CBs, we calculated the total number (Figure 7a) and number of strong (Figure 7b) C−H···X interactions per cucurbituril. Examination of the total number of interactions revealed the importance of solvation and anion coordination by CB[7] with 25 CB−Cl^- and 26 CB−water interactions per CB for only 4 CB−CB interactions that are generally weak as seen in Figure 7b (there are only a small number of strong H bonds). In the case of CB[5], the highest number of H bonds is from CB−water interactions followed by the CB−CB (8/CB) and CB−Cl^- (7/CB) interactions. But the number of strong H bonds is again very limited (equal or below 1/CB). For CB[8], it is CB−CB interactions that dominate either considering the total number of H bonds or the number of strong H bonds. Finally, the intercucurbituril network seems to be the strongest for CB[6] with a high total number *and* number of strong C−H···O interactions for structures **2** and **3**.

Thus, the observed relatively short values and high number of CH···O hydrogen bridges[43] might well be a *general* property of all cucurbituril crystals grown in aqueous acid conditions, regardless of the macrocycle size (structures **1**, **2**, **3**, and **4** plus the CB[7] one).[22] It has also been shown that they can play a critical role in molecular crystals containing glycoluril derivatives.[44,45] Moreover, Kim et al. pointed out the importance of numerous CH···O hydrogen bonds in CB[7] condensed phases with regard to its gelation behavior in acidified water.[22] Therefore, the present work demonstrates the importance of such interactions in the main representatives of the CB[*n*] family. Consequently, they may be pivotal in the understanding of the

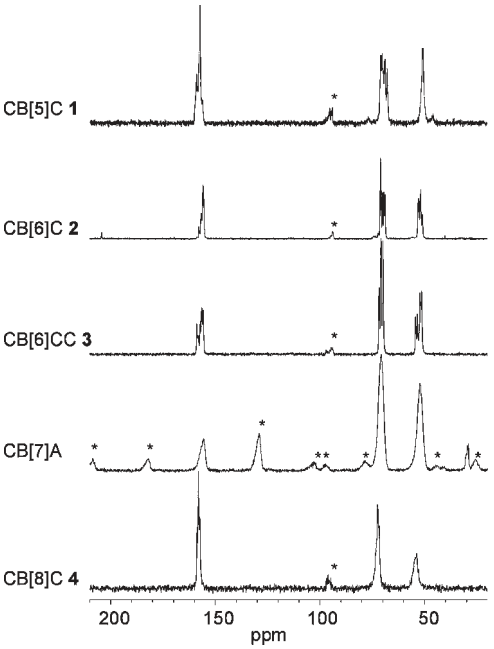

Figure 8. CP/MAS 21.1 T ^{13}C NMR spectra of CB[*n*] (*n* = 5−8) materials corresponding to crystal structures **1** CB[5]C, **2** CB[6]C, **3** CB[6]CC, and **4** CB[8]C, and amorphous CB[7]A. * indicate spinning side bands.

solid state structures and properties of cucurbiturils, for example, in explaining the surprising thermal stability of structure **3**, or their tendency to absorb water from the air, presumably to saturate the Lewis base carbonyl oxygens that are hydrogen bond demanding (see the TGA section below). The importance of CH···O interactions might be correlated to the inherent structure of the cucurbiturils and particularly the high nitrogen atom content with a proportion of 4 nitrogens for 6 carbons (general formula $C_6H_6N_4O_2$, 22% of the total atom number) possibly altering the partial charge distribution along the macrocycles. Such charge differences and peculiar nitrogen disposition (each carbon is connected to two nitrogen atoms and is thus probably electron withdrawing and therefore induces partial positive charges on the hydrogens) may enhance hydrogen bond interactions with electron rich species such as the lone pairs of neighboring cucurbituril carbonyl oxygens in a manner encountered in all the crystal structures reported here. The consequence is an *increased* acid character of the CB hydrogen atoms and an improved basic feature of the carbonyl oxygens which reinforce the H bond schemes. Thus, in effect there may be some structure-directing/-influencing information inherent to the CB molecule.

Solid State ^{13}C NMR Spectroscopy. In order to further support the solid state structures deduced by single crystal X-ray crystallography, we carried out solid state CP-MAS ^{13}C NMR experiments at 21.1 T. Also, it was hoped that ^{13}C solid state NMR spectra would prove to be a useful tool for routine characterization of CB[*n*] structures. Preliminary results obtained at 7 T showed broad featureless lines due to residual dipolar interactions with the quadrupolar ^{14}N atoms[46] (of which there are two attached to each carbon). This problem is completely eliminated at 21.1 T, resulting in spectra for the four crystalline materials which display multiple sharp resonances within three narrow regions for each of the chemically distinct carbon types: (i) C═O functions between ∼154−160 ppm,

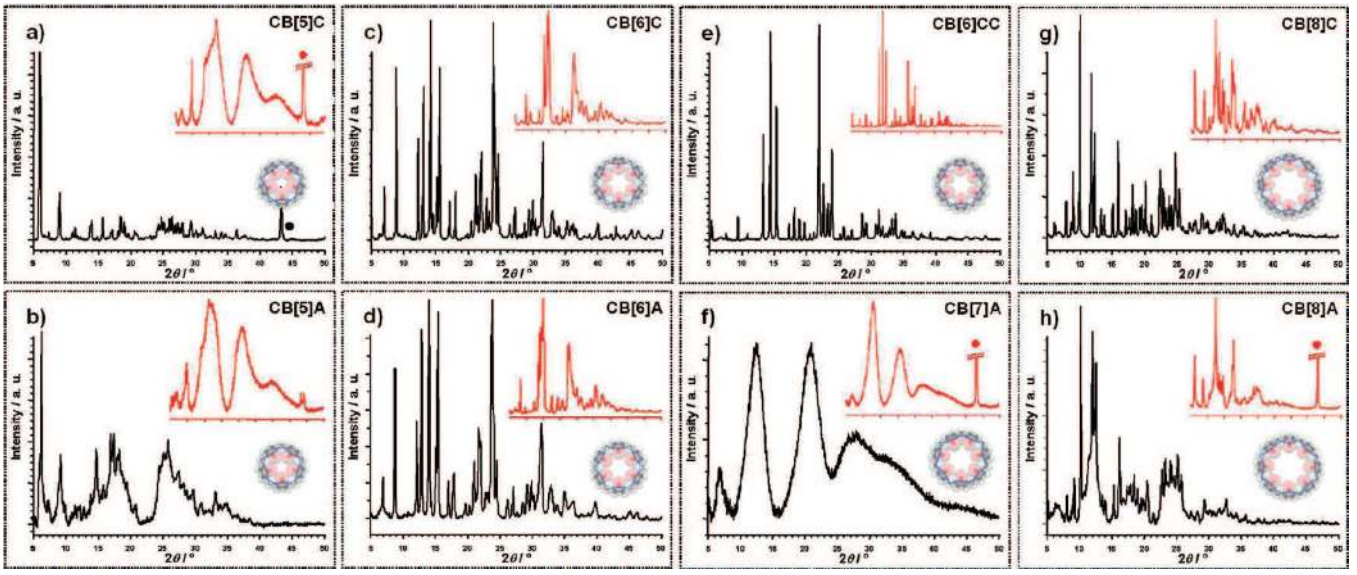

Figure 9. Powder X-ray diffractogramms of cucurbituril samples (a) **CB[5]C**, (b) **CB[5]A**, (c) **CB[6]C**, (d) **CB[6]A**, (e) **CB[6]CC**, (f) **CB[7]A**, (g) **CB[8]C**, and (h) **CB[8]A**. Insets show the resulting powder patterns of the corresponding samples treated at 100 °C for 48 h with an identical 2θ scale. ● = artifact from the sample holder.

(ii) C−H groups between ∼67−75 ppm, and (iii) bridging CH_2 groups between ∼49−57 ppm.

In the solid state chemically equivalent C atoms may have slightly different environments because of crystallographic inequivalence and thus may have small differences in chemical shift; that is, the resonance for each chemical type of carbon may be split into as many lines as there are inequivalent positions in the asymmetric unit of the crystal cell. As an example, the spectrum of **CB[6]C** shows multiplets of 2:3:1 for CH_2, 3:1:1:1 for CH, and 1:3:8 for C═O consistent with six pairs of equivalent carbons for CH_2, six pairs of equivalent carbons for CH, and four pairs of equivalent carbons plus four unique carbons for C═O as determined from the crystal structure. A more complete analysis of the lines and multiplicities will be presented elsewhere,[47] but suffice to say that in each case there is consistency between the NMR spectrum and the crystal structure. In marked contrast the spectrum of the amorphous **CB[7]A** material shows only broad featureless resonances as would be expected for a distribution of environments. The two very sharp lines seen in the spectrum of **CB[6]C** at 204.4 and 28.9 ppm confirm the presence of guest acetone molecules in this material.

One final observation from the NMR results is that dipolar dephasing[48] spectra showed complete suppression of the CH and CH_2 resonances, indicating that the CB[n] molecules are essentially static at room temperature.

Powder X-ray Diffraction (PXRD). X-ray diffraction on powdered samples was performed to determine the crystallinity of the materials before and after the thermal treatment. The powder patterns obtained for the four crystalline materials corresponding to structures **1**, **2**, **3**, and **4** (shown in Figure 9a,c,e,g) were consistent with the patterns computed from the single crystal X-ray data as can be seen in Figure S1, Supporting Information.

CB[5]A shows a crystalline pattern superimposed on an amorphous contribution (Figure 9b). The crystalline pattern has enough similarity to that of **CB[5]C**, Figure 9a, to suggest possibly the same basic structure, but there are obvious differences in line intensities. Perhaps because of the large amount of water used in the preparation of **CB[5]A**, HCl has been removed or diluted and the guest composition has been changed to mainly water.[49]

Contrary to what has been observed previously for other CB[5] crystals,[13] a 48 h thermal treatment at 100 °C resulted in complete loss of crystallinity for both samples, leading to very similar amorphous powder patterns (Figure 9a,b insets).

Although we anticipated that **CB[6]A** collected after the purification process might be amorphous, its PXRD pattern (Figure 9d) shows clearly that it is crystalline and apart from some intensity differences is very similar to the pattern of **CB[6]C** (Figure 9c). So again, although the guest content of the two materials must be different (**CB[6]A** mainly with water and **CB[6]C** with water and acetone), their basic frameworks are probably the same. Upon thermal treatment both materials produce identical patterns corresponding to a new crystalline phase (Figure 9c,d insets). In contrast, the PXRD pattern of **CB[6]CC** is largely unaffected by the same thermal treatment (Figure 9e and inset), indicating that although the guest water may be lost the structure remains intact. This is in agreement with Kim's findings with respect to the similar structure determined for CB[6] with hydrochloride[14] and confirms the remarkable stability of this particular CB[6] framework.

The pattern for **CB[7]A** confirms the amorphous nature of the as-produced material and its product after thermal treatment (Figure 9f and inset) in accord with the SCXRD and SSNMR results. The differences in intensity of the broad features probably reflect different guest content. It is noteworthy that the structures of the amorphous powder patterns in Figure 9, panels a, b, and f are quite similar. This structure perhaps reflects the fact that the individual CB molecules constitute a very small ordered array of atoms which could give rise to coherent scattering and thus give rather prominent but broad peaks in the powder pattern.

CB[8]A (Figure 9h) shows a crystalline pattern essentially the same as that of **CB[8]C** (Figure 9h),[50] superimposed on a small amount of amorphous material. Both materials transform to a

dx.doi.org/10.1021/cg201173j |*Cryst. Growth Des.* 2011, 11, 5598–5614

new crystalline phase on thermal treatment (Figure 9g,h insets), behavior reminiscent of the **CB[6]C** and **CB[6]A** cases.

As mentioned at the beginning, one of the common CB[6]-based phases which can be obtained easily is the hexagonal CB[6] *P6/mmm* structure containing water and HCl,[12] which grows directly in the reaction flask at room temperature, one or two days after the initial reaction to produce CB[*n*]s is finished. In this structure, the CB[6] molecules are found to stack on top of each other into perfect columns. These crystals very readily lose solvent, converting into the channel $R\bar{3}$ structure of Kim et al.

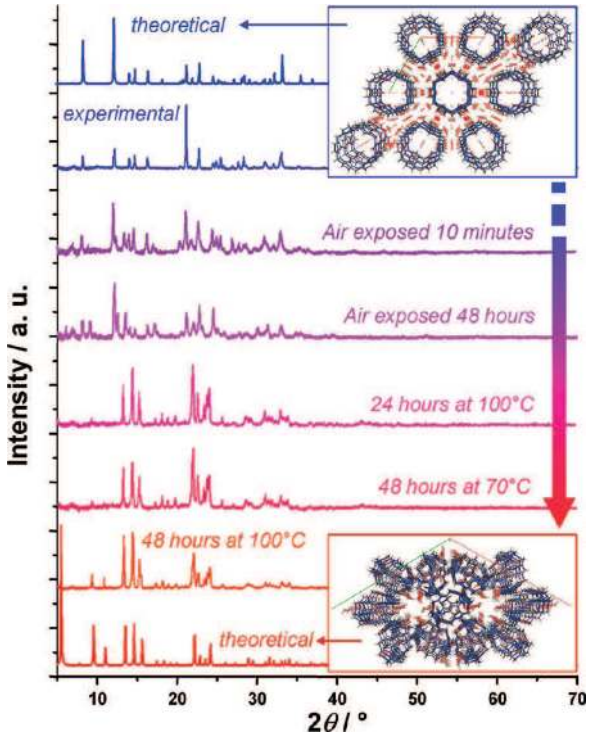

Figure 10. PXRD patterns showing the time evolution of the CB[6] *P6/mmm* structure[12] and its slow transformation to the $R\bar{3}$ (channel) structure. The process can be significantly accelerated by a suitable thermal treatment.

(**CB[6]CC**).[14] Evidence for this comes from PXRD where samples exposed to air for different lengths of time show patterns which are clearly mixtures of the *P6/mmm* and $R\bar{3}$ structures (Figure 10). Even after exposure to air at room temperature for 10 min, $R\bar{3}$ is present to a small degree. Upon heating at 70 °C for 48 h, conversion to $R\bar{3}$ is more or less complete and at 100 °C for 48 h matches the calculated pattern very well. This interpretation is also supported by ^{13}C CP/MAS NMR spectra see Figure S3, Supporting Information.

Thermogravimetric Analyses (TGA). Thermogravimetric analysis was used to evaluate the water and acid content of the eight materials as prepared, black curves of Figure 11.

The observed ~34% weight loss of **CB[5]C** crystals upon heating (Figure 11a) was in relatively good agreement with the guest content of the single crystals found by X-ray crystallography (10.88 water molecules and 3.75 HCl = 29%). It is the same situation for all the other crystalline phases for which we could derive the crystal structures (i.e., **CB[6]C**, **CB[6]CC**, and **CB[8]C**). The first ~10% of weight loss of the **CB[6]C** sample observed up to 50 °C can tentatively be assigned to the eight water molecules of the crystals (12% based on the crystal structure composition, Figure 11c). Between 50 and 340 °C, we note a small weight loss of 4% that may be due to acetone being released from the CB[6] cavity (4.8% based on the crystal structure composition) and just before the cucurbituril decomposes starting around 350 °C. Interestingly, we noted one more step in the TGA trace of **CB[6]CC** compared to that reported previously for the corresponding HCl hydrate (Figure 11e). Therefore, it seems that this structure releases its guest content *stepwise* with a first step corresponding to ~10% weight loss and a second of approximate ~9% weight loss. This could be ascribed to the successive release of the water molecules which are channel-included (and presumably more easily expelled) and inner cavity-included (presumably more difficult to release). A substantial mass decrease of ~27% was observed for **CB[8]C** up to 150 °C, probably corresponding to the 15.1 water molecules and 4 HCl per CB and thus in quite good agreement with the composition derived from the crystal structure (24% weight of guest content). Agreement between TGA and single crystal X-ray data was fairly good in all cases thereby confirming the composition of the materials. Chemical decomposition of the

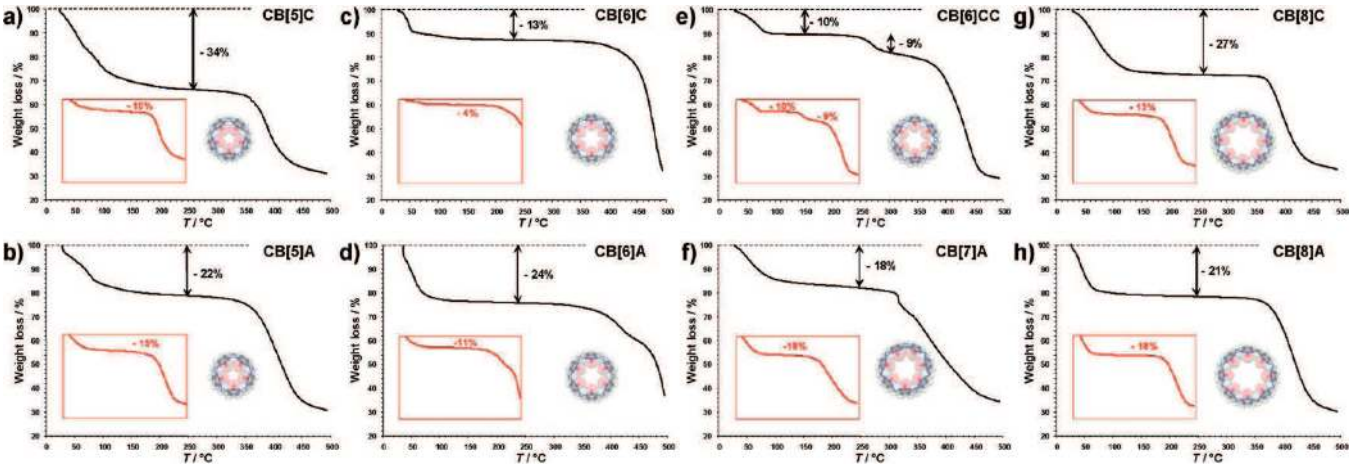

Figure 11. TGA traces of cucurbituril powdered samples of (a) **CB[5]C**, (b) **CB[5]A**, (c) **CB[6]C**, (d) **CB[6]A**, (e) **CB[6]CC**, (f) **CB[7]A**, (g) **CB[8]C**, and (h) **CB[8]A**. The red insets show the resulting TGA traces of the corresponding samples treated at 100 °C for 48 h and exposed to the air for 1 h just prior to measurements. The scale on each axis covers the same range as that of the black trace.

dx.doi.org/10.1021/cg201173j |*Cryst. Growth Des.* 2011, 11, 5598–5614

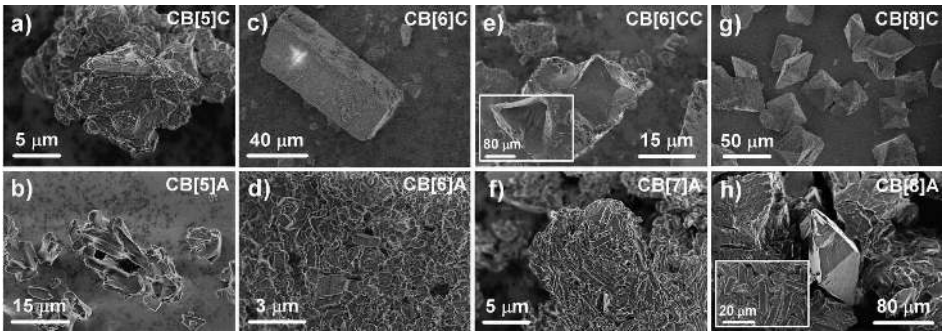

Figure 12. SEM pictures of cucurbituril powdered samples of (a) **CB[5]C**, (b) **CB[5]A**, (c) **CB[6]C**, (d) **CB[6]A**, (e) **CB[6]CC**, (f) **CB[7]A**, (g) **CB[8]C**, and (h) **CB[8]A** at room temperature. Insets show representative images of the corresponding samples after treatment at 100 °C for 48 h.

cucurbiturils was observed above 370 °C except for **CB[7]A** where decomposition began as low as 300 °C. It was also found that dried samples rapidly regained weight when left in air, presumably due to absorption of moisture. To characterize this in a consistent fashion, we subjected each of the materials to heating at 100 °C for a period of between one and two days (since all the phases appeared to lose their guest content when reaching 100 °C), followed by air exposure for 1 h. TGA was then immediately scanned from room temperature up to 500 °C (TGA red traces as insets in Figure 11 for the corresponding samples, everything with an identical tare). All the powders *gained* weight after the period of air exposure and the red TGA traces show rapid mass decrease up to ∼100−120 °C. Even for the smallest weight gain of approximately 4% weight, this could mean that two water molecules per cucurbituril have been complexed. Elemental analysis for a sample of **CB[6]A** after the same treatment of drying and air exposure is consistent with the TGA data (Figure 11d inset) provided some residual HCl content is assumed: 1.8 HCl and 3 H_2O molecules per CB (calculated [found]: H 3.95 [4.03], C 38.72 [38.89], N 30.10 [29.99]) accounting for ≈10.7% of the total mass (as compared with 11% on the red trace). Similarly for **CB[7]A**, the elemental analysis and a guest content of 3.2 HCl and 5.6 H_2O molecules per CB (calculated [found]: H 4.12 [4.60], C 36.53 [36.25], N 28.40 [28.68]) are consistent with the TGA result (Figure 11f inset) with a mass content for the guests of ≈15.8% (to be compared with 18% on the red trace). Residual HCl content is also in accord with the low pH values recorded for dissolved or suspended CB powders in water.[20] The TGA plots show a very slight negative slope in the 100−300 °C region that may be attributed to release of remaining HCl. It therefore appears that heating at 100 °C only expels water from the powders, and re-exposure to air results in the CBs reabsorbing some water to the level shown in Figure 11 (red traces). This strong tendency to *reabsorb* water from the atmosphere after drying must be kept in mind when considering CBs for such applications as gas adsorption.[14,51]

Scanning Electron Microscopy. SEM was performed to investigate the sample micromorphology before and after thermal treatment (Figure 12). **CB[5]C** did not show any distinct crystals, but crystallinity is evident from the straight lines and layering that can be seen in most of the pictures (Figure 12a). **CB[5]A** was clearly *amorphous* on this scale (Figure 12b) with no clear evidence of the crystalline fraction indicated by the PXRD (see Figure 9b).

Conversely, **CB[6]C** clearly shows sizable crystals (Figure 12c) that can survive the heating treatment (numerous cracks can be seen in this case), in line with PXRD (Figure 9c). **CB[6]A** prepared using ultrasound (Figure 12d) shows mainly a fine texture without any regular shapes with a few much smaller slab-like crystals, consistent with PXRD. This is remarkable considering the harsh ultrasound treatment and further proves the strong tendency of CB[6] to self-assemble and ultimately crystallize according to structure **2** (see Figure 2).[52] **CB[6]CC** exhibited some crystalline morphologies with flat sharp surfaces (Figure 12e) also in agreement with PXRD. While some cracks were also clearly visible after the applied thermal treatment (inset) the crystals survived. **CB[7]A** (Figure 12f) does not show any facets or layering that would indicate any crystallinity, and the topography is reminiscent of the microstructure of the kind of assemblies found for bad gelators[53] (long entangled ribbons have been observed in CB[7] gels derived from hot acidic aqueous solutions).[22] This reflects again the tendency of CB[7] to self-assemble but in a manner more favorable to the formation of gels than for crystal growth as often mentioned in the literature for this type of behavior (good gelators rarely crystallize).[53,54] In this case, PXRD is complementary to SEM in identifying the structure as amorphous (see powder pattern of Figure 9f). **CB[8]C** shows flattened *octahedral* microcrystals, similar to larger crystals observed visually (Figure 12g), whereas **CB[8]A** showed the same octahedral crystals together with irregular shapes (Figure 12h). Elongated *prism-like* crystals with rounded edges were observed after applying the thermal treatment (inset Figure 12h). Thus, SEM pictures generally correlate well at the micrometer scale with the PXRD results.

■ CONCLUSION

The combination of solid state techniques (SCXRD, SSNMR, PXRD, TGA, and SEM) has provided a unique set of self-consistent information for the structural assessment of CB[*n*] materials. Collectively, the results of this *solid state* approach allow for a better understanding of physical properties such as the solubility, crystallinity, and thermal stability for samples which are quite representative of the types one can obtain after purification. Of particular interest is the ability of the cucurbiturils to organize themselves in the solid state in such a way that one CB closes off one side of the cavity of another CB (partially self-closing) in a motif reminiscent of a *cross*. Indeed, in the absence of stronger competing interactions (ion−dipole for example via metal coordination such as Na, K, Rb, Cs, ...)[55] the CBs tend to self-associate forming 1D chains (CB[5] structure **1** and CB[6] structure **2**, which are half self-closed) and three-dimensional networks (CB[6] structure **3** and CB[8] structure **4** which are

fully self-closed) according to this *cross* motif. We were able to shed some light on the delicate balance of the weak interactions in cucurbituril crystals and propose that the multiplicity of cucurbituril CH···O interactions is the essence of their stability (or at least is the structure directing factor), which might also explain why CBs tend to aggregate in water.[10,11] All the CB[*n*] materials investigated here transform to another phase upon heating except for **CB[6]CC**, which retains its original channel structure, and **CB[7]A**, which is always amorphous. It is likely that when water is released by the thermal treatment, this allows a better closure or self-penetration of the cavities, thus restricting empty space in a more dense phase and maximizing the number of stabilizing CH···O interactions on a *per CB* basis. It was established that CB[5] and CB[7] based powders are amorphous after drying, whereas CB[6] and CB[8] related powders are still crystalline. We propose that the observed odd−even effect in the CB crystallinity (especially after thermal treatment), and perhaps also water solubility and micromorphology, can be simply and solely explained by symmetry arguments, that is, a less efficient self-association for CB[5] and CB[7] as compared with CB[6] and CB[8], resulting in fewer CH···O interactions *per cucurbituril*. This would lead to a more favorable solvation for the CBs having an odd symmetry whereas those having an even one would prefer to self-associate in a manner ultimately leading to crystallization. We also showed that the hexagonal CB[6] *P6/mmm* crystals (perfect stack structure) slowly transform (faster with the aid of heat) to the channel microporous crystals of CB[6] $R\bar{3}$ form, which shows much promise for gas storage. We believe that this is an important and facile route for the bulk preparation of the CB[6]-$R\bar{3}$ material because of the ease of crystal growth (very large hexagonal crystals of CB[6] grow directly inside the reaction flask at the end of the synthesis reaction) and its high potential for scale up (17 g were obtained for the best batch of crystals). Finally, cucurbituril solids were also demonstrated to be *moisture sensitive* with a rapid water adsorption (≥4% by weight) after thermal activation. Besides, these findings are important because they provide a structural basis accounting for intriguing yet unexplained aspects of cucurbituril solid and liquid state properties. One general observation which has emerged is that the CB[*n*] form a plethora of different host−guest structural types, where the frameworks can change markedly depending on the ring size and the guest and water content. However, as the number of crystal structures increases it is becoming apparent that certain structural types occur more than once (the same crystal framework with different guests), e.g., the CB[6] $R\bar{3}$ structure (this work and Kim's structure);[14] the **CB[6]C** Cmc21 structure (this work and a recent work on a diethyl ether/water complex);[28] the CB[8] I41/a structure (this work and refs 2c and 7m). Beyond the structural insights gained from the combination of techniques employed, this paper provides a convenient overview for the preparation and use of CB[*n*] materials with well-defined, unequivocal structures. This may help expand the use of these synthetic and appealing macrocycles in advanced applications such as self-sorting systems,[56] adaptive chemistry,[57] systems chemistry,[58] and for gas adsorption.[14]

■ ASSOCIATED CONTENT

Supporting Information. Additional PXRD patterns, SEM images, and solid state ^{13}C NMR spectra. This information is available free of charge via the Internet at http://pubs.acs.org.

■ AUTHOR INFORMATION

Corresponding Author

*E-mail: (D.B)david.bardelang@univ-provence.fr; tel: 00 33 491 288 610; fax: 00 33 491 288 758. E-mail: (C.I.R.)christopher.ratcliffe@nrc-cnrc.gc.ca.

Present Addresses

#Faculté des Sciences de Saint-Jérôme, case 521 Equipe SREP, UMR-6264, Laboratoire Chimie Provence Avenue Escadrille Normandie-Niemen 13397 Marseille Cedex 20, France.

■ ACKNOWLEDGMENT

We would like to thank Mélanie Waite and Victor Terskikh for their kind help with the CB samples. We also thank the National Research Council of Canada for financial support. Access to the 900 MHz NMR spectrometer was provided by the National Ultrahigh Field NMR Facility for Solids (Ottawa, Canada), a national research facility funded by the Canada Foundation for Innovation, the Ontario Innovation Trust, Recherche Québec, the National Research Council Canada, and Bruker BioSpin and managed by the University of Ottawa (http://www.nmr900.ca).

■ REFERENCES

(1) (a) Gerasko, O. A.; Samsonenko, D. G.; Fedin, V. P. *Russ. Chem. Rev.* **2002**, *71*, 741–760. (b) Lee, J. W.; Samal, S.; Selvapalam, N.; Kim, H.-J.; Kim, K. *Acc. Chem. Res.* **2003**, *36*, 621–630. (c) Lagona, J.; Mukhopadhyay, P.; Chakrabarti, S.; Isaacs, L. *Angew. Chem., Int. Ed.* **2005**, *44*, 4844–4870. (d) Isaacs, L. *Chem. Commun.* **2009**, 619–629.

(2) (a) Freeman, W. A.; Mock, W. L.; Shih, N.-Y. *J. Am. Chem. Soc.* **1981**, *103*, 7367–7368. (b) Flinn, A.; Hough, G. C.; Stoddart, J. F.; Williams, D. J. *Angew. Chem., Int. Ed. Engl.* **1992**, *31*, 1475–1477. (c) Kim, J.; Jung, I.-S.; Kim, S.-Y.; Lee, E.; Kang, J.-K.; Sakamoto, S.; Yamaguchi, K.; Kim, K. *J. Am. Chem. Soc.* **2000**, *122*, 540–541. (d) Day, A.; Arnold, A. P.; Blanch, R. J.; Snushall, B. *J. Org. Chem.* **2001**, *66*, 8094–8100. (e) Zhao, J.; Kim, H.-J.; Oh, J.; Kim, S.-Y.; Lee, J. W.; Sakamoto, S.; Yamaguchi, K.; Kim, K. *Angew. Chem., Int. Ed.* **2001**, *40*, 4233–4235. (f) Isobe, H.; Sato, S.; Nakamura, E. *Org. Lett.* **2002**, *4*, 1287–1289. (g) Jon, S. Y.; Selvapalam, N.; Oh, D. H.; Kang, J.-K.; Kim, S.-Y.; Jeon, Y. J.; Lee, J. W.; Kim, K. *J. Am. Chem. Soc.* **2003**, *125*, 10186–10187. (h) Day, A. I.; Arnold, A. P.; Blanch, R. J. *Molecules* **2003**, *8*, 74–84. (i) Miyahara, Y.; Goto, K.; Oka, M.; Inazu, T. *Angew. Chem., Int. Ed.* **2004**, *43*, 5019–5022. (j) Liu, S.; Zavalij, P. Y.; Isaacs, L. *J. Am. Chem. Soc.* **2005**, *127*, 16798–16799. (k) Isaacs, L.; Park, S.-K.; Liu, S.; Ko, Y. H.; Selvapalam, N.; Kim, Y.; Kim, H.; Zavalij, P. Y.; Kim, G.-H.; Lee, H.-S.; Kim, K. *J. Am. Chem. Soc.* **2005**, *127*, 18000–18001. (l) Huang, W.-H.; Liu, S.; Zavalij, P. Y.; Isaacs, L. *J. Am. Chem. Soc.* **2006**, *128*, 14744–14745. (m) Huang, W.-H.; Zavalij, P. Y.; Isaacs, L. *Angew. Chem., Int. Ed.* **2007**, *46*, 7425–7427. (n) Kim, J.; Ahn, Y.; Park, K. M.; Kim, Y.; Ko, Y. H.; Oh, D. H.; Kim, K. *Angew. Chem., Int. Ed.* **2007**, *46*, 7393–7395. (o) Kim, K.; Selvapalam, N.; Ko, Y. H.; Park, K. M.; Kim, D.; Kim, J. *Chem. Soc. Rev.* **2007**, *36*, 267–279. (p) Ni, X.-L.; Lin, J.-X.; Zheng, Y.-Y.; Wu, W.-S.; Zhang, Y.-Q.; Xue, S.-F.; Zhu, Q.-J.; Tao, Z.; Day, A. I. *Cryst. Growth Des.* **2008**, *8*, 3446–3450. (q) Tian, Z.-C.; Ni, X.-L.; Xiao, X.; Wu, F.; Zhang, Y.-Q.; Zhu, Q.-J.; Xue, S.-F.; Tao, Z. *J. Mol. Struct.* **2008**, *888*, 48–54. (r) Yu, D.-H.; Ni, X.-L.; Tian, Z.-C.; Zhang, Y.-Q.; Xue, S.-F.; Tao, Z.; Zhu, Q.-J. *J. Mol. Struct.* **2008**, *891*, 247–253. (s) Zheng, L.-M.; Zhang, Y.-Q.; Zeng, J.-P.; Qiu, Y.; Yu, D.-H.; Xue, S.-F.; Zhu, Q.-J.; Tao, Z. *Molecules* **2008**, *13*, 2814–2822. (t) Huang, W.-H.; Zavalij, P. Y.; Isaacs, L. *Org. Lett.* **2008**, *10*, 2577–2580. (u) Zhou, F.-G.; Wu, L.-H.; Lu, X.-J.; Zhang, Y.-Q.; Zhu, Q.-J.; Xue, S.-F.; Tao, Z. *J. Mol. Struct.* **2009**, *927*, 14–20. (v) Chen, Z.-H.; Zhou, F.-G.; Zhang, Y.-Q.; Zhu, Q.-J.; Xue, S.-F.; Tao, Z. *J. Mol. Struct.* **2009**, *930*, 140–146. (w) Zhang, Y.-Q.; Zeng, J.-P.; Zhu, Q.-J.; Xue, S.-F.; Tao, Z. *J. Mol. Struct.*

2009, *929*, 167–173. (x) Wu, L.-H.; Ni, X.-L.; Wu, F.; Zhang, Y.-Q.; Zhu, Q.-J.; Xue, S.-F.; Tao, Z. *J. Mol. Struct.* **2009**, *920*, 183–188.

(3) (a) Rekharsky, M. V.; Mori, T.; Yang, C.; Ko, Y. H.; Selvapalam, N.; Kim, H.; Sobransingh, D.; Kaifer, A. E.; Liu, S.; Isaacs, L.; Chen, W.; Moghaddam, S.; Gilson, M. K.; Kim, K.; Inoue, Y. *Proc. Natl. Acad. Sci. U. S. A.* **2007**, *104*, 20737–20742. (b) Hwang, I.; Baek, K.; Jung, M.; Kim, Y.; Park, K. M.; Lee, D.-W.; Selvapalam, N.; Kim, K. *J. Am. Chem. Soc.* **2007**, *129*, 4170–4171. (c) Moghaddam, S.; Inoue, Y.; Gilson, M. K. *J. Am. Chem. Soc.* **2009**, *131*, 4012–4021.

(4) (a) Kim, K. *Chem. Soc. Rev.* **2002**, *31*, 96–107and references therein. (b) Park, K.-M.; Kim, S.-Y.; Heo, J.; Whang, D.; Sakamoto, S.; Yamaguchi, K.; Kim, K. *J. Am. Chem. Soc.* **2002**, *124*, 2140–2147. (c) Park, K.-M.; Roh, S.-G.; Lee, E.; Kim, J.; Kim, H.-J.; Lee, J. W.; Kim, K. *Supramol. Chem.* **2002**, *14*, 153–158. (d) Ko, Y. H.; Kim, K.; Kang, J.-K.; Chun, H.; Lee, J. W.; Sakamoto, S.; Yamaguchi, K.; Fettinger, J. C.; Kim, K. *J. Am. Chem. Soc.* **2004**, *126*, 1932–1933. (e) Kim, S.-Y.; Ko, Y. H.; Lee, J. W.; Sakamoto, S.; Yamaguchi, K.; Kim, K. *Chem. Asian J.* **2007**, *2*, 747–754. (f) Ke, C.-F.; Hou, S.; Zhang, H.-Y.; Liu, Y.; Yang, K.; Feng, X.-Z. *Chem. Commun.* **2007**, 3374–3376. (g) Rauwald, U.; Scherman, O. A. *Angew. Chem., Int. Ed.* **2008**, *47*, 3950–3953. (h) Tuncel, D.; Katterle, M. *Chem.—Eur. J.* **2008**, *14*, 4110–4116. (i) Ko, Y. H.; Kim, H.; Kim, Y.; Kim, K. *Angew. Chem., Int. Ed.* **2008**, *47*, 4106–4109. (j) Wang, W.; Kaifer, A. E. *Adv. Polym. Sci.* **2009**, *222*, 205–235. (k) Nally, R.; Isaacs, L. *Tetrahedron* **2009**, *65*, 7249–7258. (l) Jayaraj, N.; Porel, M.; Ottaviani, M. F.; Maddipatla, M. V. S. N.; Modelli, A.; Da Silva, J. P.; Bhogala, B. R.; Captain, B.; Jockusch, S.; Turro, N. J.; Ramamurthy, V. *Langmuir* **2009**, *25*, 13820–13832. (m) Mileo, E.; Mezzina, E.; Grepioni, F.; Pedulli, G. F.; Lucarini, M. *Chem . Eur. J.* **2009**, *15*, 7859–7862.

(5) (a) Lee, J. W.; Kim, K.; Kim, K. *Chem. Commun.* **2001**, 1042–1043. (b) Day, A. I.; Blanch, R. J.; Arnold, A. P.; Lorenzo, S.; Lewis, G. R.; Dance, I. *Angew. Chem., Int. Ed.* **2002**, *41*, 275–277. (c) Blanch, R. J.; Sleeman, A. J.; White, T. J.; Arnold, A. P.; Day, A. I. *Nano Lett.* **2002**, *2*, 147–149. (d) Jeon, W. S.; Ziganshina, A. Y.; Lee, J. W.; Ko, Y. H.; Kang, J.-K.; Lee, C.; Kim, K. *Angew. Chem., Int. Ed.* **2003**, *42*, 4097–4100. (e) Jeon, W. S.; Kim, E.; Ko, Y. H.; Hwang, I.; Lee, J. W.; Kim, S.-Y.; Kim, H.-J.; Kim, K. *Angew. Chem., Int. Ed.* **2005**, *44*, 87–91. (f) Ko, Y. H.; Kim, E.; Hwang, I.; Kim, K. *Chem. Commun.* **2007**, 1305–1315. (g) Sindelar, V.; Silvi, S.; Parker, S. E.; Sobransingh, D.; Kaifer, A. E. *Adv. Funct. Mater.* **2007**, *17*, 694–701. (h) Tuncel, D.; Özsar, Ö.; Tiftik, H. B.; Salih, B. *Chem. Commun.* **2007**, 1369–1371. (i) Angelos, S.; Yang, Y.-W.; Patel, K.; Stoddart, J. F.; Zink, J. I. *Angew. Chem., Int. Ed.* **2008**, *47*, 2222–2226. (j) Ben Shir, I.; Sasmal, S.; Mejuch, T.; Sinha, M. K.; Kapon, M.; Keinan, E. *J. Org. Chem.* **2008**, *73*, 8772–8779. (k) Khashab, N. M.; Trabolsi, A.; Lau, Y. A.; Ambrogio, M. W.; Friedman, D. C.; Khatib, H. A.; Zink, J. I.; Stoddart, J. F. *Eur. J. Org. Chem.* **2009**, *11*, 1669–1673. (l) Hwang, I.; Ziganshina, A. Y.; Ko, Y. H.; Yun, G.; Kim, K. *Chem. Commun.* **2009**, 416–418. (m) Angelos, S.; Yang, Y.-W.; Khashab, N. M.; Stoddart, J. F.; Zink, J. I. *J. Am. Chem. Soc.* **2009**, *131*, 11344–11346. (n) Angelos, S.; Khashab, N. M.; Yang, Y.-W.; Trabolsi, A.; Khatib, H. A.; Stoddart, J. F.; Zink, J. I. *J. Am. Chem. Soc.* **2009**, *131*, 12912–12914.

(6) (a) Buschmann, H.-J.; Schollmeyer, E.; Mutihac, L. *Thermochim. Acta* **2003**, *399*, 203–208. (b) Bush, M. E.; Bouley, N. D.; Urbach, A. R. *J. Am. Chem. Soc.* **2005**, *127*, 14511–14517. (c) Heitmann, L. M.; Taylor, A. B.; Hart, P. J.; Urbach, A. R. *J. Am. Chem. Soc.* **2006**, *128*, 12574–12581. (d) Rekharsky, M. V.; Yamamura, H.; Inoue, C.; Kawai, M.; Osaka, I.; Arakawa, R.; Shiba, K.; Sato, A.; Ko, Y. H.; Selvapalam, N.; Kim, K.; Inoue, Y. *J. Am. Chem. Soc.* **2006**, *128*, 14871–14880. (e) Rekharsky, M. V.; Yamamura, H.; Ko, Y. H.; Selvapalam, N.; Kim, K.; Inoue, Y. *Chem. Commun.* **2008**, 2236–2238. (f) Bailey, D. M.; Hennig, A.; Uzunova, V. D.; Nau, W. M. *Chem.—Eur. J.* **2008**, *14*, 6069–6077. (g) Zhang, H.; Grabenauer, M.; Bowers, M. T.; Dearden, D. V. *J. Phys. Chem. A* **2009**, *113*, 1508–1517. (h) Reczek, J. J.; Kennedy, A. A.; Halbert, B. T.; Urbach., A. R. *J. Am. Chem. Soc.* **2009**, *131*, 2408–2415.

(7) (a) Wheate, N. J.; Day, A. I.; Blanch, R. J.; Arnold, A. P.; Cullinane, C.; Collins, J. G. *Chem. Commun.* **2004**, 1424–1425. (b) Jeon, Y. J.; Kim, S.-Y.; Ko, Y. H.; Sakamoto, S.; Yamaguchi, K.; Kim, K. *Org. Biomol. Chem.* **2005**, *3*, 2122–2125. (c) Wheate, N. J.; Buck, D. P.; Day, A. I.; Collins, J. G. *Dalton Trans.* **2006**, *3*, 451–458. (d) Bali, M. S.; Buck, D. P.; Coe, A. J.; Day, A. I.; Collins, J. G. *Dalton Trans.* **2006**, *45*, 5337–5344. (e) Kemp, S.; Wheate, N. J.; Wang, S.; Collins, J. G.; Ralph, S. F.; Day, A. I.; Higgins, V. J.; Aldrich-Wright, J. R. *J. Biol. Inorg. Chem.* **2007**, *12*, 969–979. (f) Wheate, N. J.; Taleb, R. I.; Krause-Heuer, A. M.; Cook, R. L.; Wang, S.; Higgins, V. J.; Aldrich-Wright, J. R. *Dalton Trans.* **2007**, *43*, 5055–5064. (g) Zhao, Y.; Buck, D. P.; Morris, D. L.; Pourgholami, M. H.; Day, A. I.; Collins, J. G. *Org. Biomol. Chem.* **2008**, *6*, 4509–4515. (h) Buck, D. P.; Abeysinghe, P. M.; Cullinane, C.; Day, A. I.; Collins, J. G.; Harding, M. M. *Dalton Trans.* **2008**, *17*, 2328–2334. (i) Wang, R.; Macartney, D. H. *Org. Biomol. Chem.* **2008**, *6*, 1955–1960. (j) Saleh, N.; Koner, A. L.; Nau, W. N. *Angew. Chem., Int. Ed.* **2008**, *47*, 5398–5401. (k) Dong, N.; Xue, S.-F.; Zhu, Q.-J.; Tao, Z.; Zhao, Y.; Yang, L.-X. *Supramol. Chem.* **2008**, *20*, 663–671. (l) Wheate, N. J. *J. Inorg. Biochem.* **2008**, *102*, 2060–2066. (m) Wang, R.; Bardelang, D.; Waite, M.; Udachin, K. A.; Leek, D. M.; Yu, K.; Ratcliffe, C. I.; Ripmeester, J. A. *Org. Biomol. Chem.* **2009**, *7*, 2435–2439. (n) Zhao, Y.; Bali, M. S.; Cullinane, C.; Day, A. I.; Collins, J. G. *Dalton Trans.* **2009**, *26*, 5190–5198. (o) Kennedy, A. R.; Florence, A. J.; McInnes, F. J.; Wheate, N. J. *Dalton Trans.* **2009**, *37*, 7695–7700. (p) Wang, R.; MacGillivray, B. C.; Macartney, D. H. *Dalton Trans.* **2009**, *18*, 3584–3589. (q) Montes-Navajas, P.; Gonzalez-Béjar, M.; Scaiano, J. C.; Garcia, H. *Photochem. Photobiol. Sci.* **2009**, *8*, 1743–1747. (r) Wyman, I. W.; Macartney, D. H. *Org. Biomol. Chem.* **2010**, *8*, 247–252. (s) Wyman, I. W.; Macartney, D. H. *Org. Biomol. Chem.* **2010**, *8*, 253–260. (t) Uzunova, V. D.; Cullinane, C.; Brix, K.; Nau, W. M.; Day, A. I. *Org. Biomol. Chem.* **2010**, *8*, 2037–2042.

(8) Huang, W.-H.; Zavalij, P. Y.; Isaacs, L. *J. Am. Chem. Soc.* **2008**, *130*, 8446–8454.

(9) Crystal structures of CB[6] have been reported in the seminal work of Mock and Shih (see ref 2a) and that reported later by Freeman (see following), but was shown to be different from that reported here: Freeman, W. A. *Acta Crystallogr. Sect. B* **1984**, *40*, 382–387. A columnar CB[8] structure has been reported recently with perchlorate as structural unit with each macrocycles deviating from perfect alignment:Kuz'mina, L. G.; Vedernikov, A. I.; Lobova, N. A.; Howard, J. A. K.; Strelenko, Y. A.; Fedin, V. P.; Alfimov, M. V.; Gromov, S. P. *New J. Chem.* **2006**, *30*, 458–466.

(10) (a) Wheate, N. J.; Anil Kumar, P. G.; Torres, A. M.; Aldrich-Wright, J. R.; Price, W. S. *J. Phys. Chem. B* **2008**, *112*, 2311–2314. (b) Grant, M. P.; Wheate, N. J.; Aldrich-Wright, J. R. *J. Chem. Eng. Data* **2009**, *54*, 323–326. (c) Da Silva, J. P.; Jayaraj, N.; Jockusch, S.; Turro, N. J.; Ramamurthy, V. *Org. Lett.* **2011**, *13*, 2410–2413.

(11) Bardelang, D.; Banaszak, K.; Karoui, H.; Rockenbauer, A.; Waite, M.; Udachin, K.; Ripmeester, J. A.; Ratcliffe, C. I.; Ouari, O.; Tordo, P. *J. Am. Chem. Soc.* **2009**, *131*, 5402–5404.

(12) Bardelang, D.; Udachin, K. A.; Leek, D. M.; Ripmeester, J. A. *CrystEngComm* **2007**, *9*, 973–975.

(13) Bardelang, D.; Udachin, K. A.; Anedda, R.; Moudrakovski, I.; Leek, D. M.; Ripmeester, J. A.; Ratcliffe, C. I. *Chem. Commun.* **2008**, 4927–4929.

(14) Lim, S.; Kim, H.; Selvapalam, N.; Kim, K.-J.; Cho, S. J.; Seo, G.; Kim, K. *Angew. Chem., Int. Ed.* **2008**, *47*, 3352–3355.

(15) (a) Taylor, R.; Kennard, O. *J. Am. Chem. Soc.* **1982**, *104*, 5063–5070. (b) Desiraju, G. R. *Acc. Chem. Res.* **1991**, *24*, 290–296. (c) Desiraju, G. R. *Acc. Chem. Res.* **1996**, *29*, 441–449. (d) Castellano, R. K. *Curr. Org. Chem.* **2004**, *8*, 845–865.

(16) Steiner, T. *Angew. Chem., Int. Ed.* **2002**, *41*, 48–76.

(17) (a) Lehn, J.-M. *Supramolecular Chemistry*; Wiley-VCH: Weinheim, 1995. (b) Steed, J. W.; Atwood, J. L. *Supramolecular Chemistry*; Wiley-VCH: London, 2000.

(18) Wu, X.-J.; Hu, K.; Meng, X.-G.; Cheng, G.-Z. *New J. Chem.* **2010**, *34*, 17–20.

(19) An, Q.; Chen, Q.; Zhu, W.; Li, Y.; Tao, C.-A.; Yang, H.; Li, Z.; Wan, L.; Tian, H.; Li, G. *Chem. Commun.* **2010**, *46*, 725–727.

(20) The tendency of cucurbiturils to retain acid derivatives is a well-known property, and one should take note of the pH when running

host·guest binding studies. In our case, we could not completely get rid of all the acid, as even after several washes using ultrasound the pH of resuspended CB[6] was still around 4: (a) Neugebauer, R.; Knoche, W. *J. Chem. Soc., Perkin Trans. 2* **1998**, *3*, 529–534. (b) Bernal, I.; Mukhopadhyay, U.; Virovets, A. V.; Fedin, V. P.; Clegg, W. *Chem. Commun.* **2005**, 3791–3792.

(21) While searching these small white needles for suitable crystals for structural determination, we discovered that another phase was present in a very low proportion (<2%). Single crystal X-ray diffraction on this material showed it to be the CB[5]@CB[10] structure previously given in a preliminary report.[5b] Powder X-ray diffraction of a sample originating from a large set of crystals displayed the expected diffraction peaks of the CB[6]-based structure **2**, whereas those related to the CB[5]@CB[10] structure were hardly detectable.

(22) Hwang, I.; Jeon, W. S.; Kim, H.-J.; Kim, D.; Kim, H.; Selvapalam, N.; Fujita, N.; Shinkai, S.; Kim, K. *Angew. Chem., Int. Ed.* **2007**, *46*, 210–213.

(23) Sheldrick, G. M. *SADABS*, Version 2.03; University of Gottingen: Germany, 2002.

(24) Sheldrick, G. M. *SHELXTL*, Version 6.10; Bruker AXS Inc.: Madison, Wisconsin, USA, 2000.

(25) Thuéry, P. *Cryst. Growth Des.* **2008**, *8*, 4132–4143. And for papers that reported *partial* cucurbituril self-closing together with other interaction modes see:(a) Lorenzo, S.; Day, A.; Craig, D.; Blanch, R.; Arnold, A.; Dance, I. *CrystEngComm* **2001**, *49*, 1–7. (b) Samsonenko, D. G.; Lipkowski, J.; Gerasko, O. A.; Virovets, A. V.; Sokolov, M. N.; Fedin, V. P.; Platas, J. G.; Hernandez-Molina, R.; Mederos, A. *Eur. J. Inorg. Chem.* **2002**, *9*, 2380–2388. (c) Gerasko, O. A.; Mainicheva, E. A.; Naumova, M. I.; Yurjeva, O. P.; Alberola, A.; Vicent, C.; Llusar, R.; Fedin, V. P. *Eur. J. Inorg. Chem.* **2008**, *3*, 416–424. (d) Gerasko, O. A.; Mainicheva, E. A.; Naumova, M. I.; Neumaier, M.; Kappes, M. M.; Lebedkin, S.; Fenske, D.; Fedin, V. P. *Inorg. Chem.* **2008**, *47*, 8869–8880. (e) Thuéry, P. *Cryst. Growth Des.* **2009**, *9*, 1208–1215. (f) Thuéry, P. *CrystEngComm* **2009**, *11*, 1150–1156.

(26) A great deal of work has been reported in the literature concerning cucurbituril-containing solid state structures by the group of Fedin; see for example refs 1a 25b 25c 25d, and (a) Sokolov, M. N.; Dybtsev, D. N.; Fedin, V. P. *Russ. Chem. Bull., Int. Ed.* **2003**, *52*, 1041–1060and references therein. (b) Gerasko, O. A.; Virovets, A. V.; Samsonenko, D. G.; Tripolskaya, A. A.; Fedin, V. P.; Fenske, D. *Russ. Chem. Bull., Int. Ed.* **2003**, *52*, 585–593. (c) Gerasko, O. A.; Sokolov, M. N.; Fedin, V. P. *Pure Appl. Chem.* **2004**, *76*, 1633–1646See also ref 55.

(27) Liu, S.-M.; Huang, Z.-X.; Wu, X.-J.; Liang, F.; Wu, C.-T. *Chin. J. Chem.* **2004**, *22*, 1208–1210.

(28) Liu, L.; Nouvel, N.; Scherman, O. A. *Chem. Commun.* **2009**, 3243–3245.

(29) However, we expect the acetone hydrogen to carry a partial positive charge (contrary to the chloride anion of structure **1**). In this case, the occurrence of such a strong contact in the acetone complex of structure **2** may appear contradictory to our hypothesis given for the chloride encapsulation (double-crown of electropositive carbons). However, the fact that the rigid CB[6] macrocycle is quite distorted after having included acetone can be a sign of some steric strain upon inclusion. Thus the driving force of guest inclusion is likely to be mostly due to the hydrophobic effect but at the expense of a small steric strain responsible for the macrocycle deformation. This can also tentatively be paralleled with orthogonal dipolar C═O···C═O interactions that are well documented in the literature. See for example: Fäh, C.; Hardegger, L. A.; Ebert, M.-O.; Schweizer, B.; Diederich, F. *Chem. Commun.* **2010**, *46*, 67–69.

(30) We note that we never obtained bulk CB[6] as pure as found in the crystal structures, since ^{1}H NMR showed the presence of a very small amount of *i*CB[6] that we could not remove.

(31) (a) MacDonald, J. C.; Whitesides, G. M. *Chem. Rev.* **1994**, *94*, 2383–2420. (b) Philp, D.; Stoddart, J. F. *Angew. Chem., Int. Ed. Engl.* **1996**, *35*, 1154–1196. (c) Lehn, J.-M. *Chem.—Eur. J.* **2000**, *6*, 2097–2102. (d) Whitesides, G. M.; Grzybowski, B. *Science* **2002**, *295*, 2418–2421.

(32) Introduction of Hirshfeld surfaces, graphical tools and relevant examples:(a) Spackman, M. A.; Byrom, P. G. *Chem. Phys. Lett.* **1997**, *267*, 215–220. (b) McKinnon, J. J.; Mitchell, A. S.; Spackman, M. A. *Chem.—Eur. J.* **1998**, *4*, 2136–2141. (c) Spackman, M. A.; McKinnon, J. J. *CrystEngComm* **2002**, *4*, 378–392. (d) McKinnon, J. J.; Spackman, M. A.; Mitchell, A. S. *Acta Crystallogr., Sect. B* **2004**, *60*, 627–668. (e) McKinnon, J. J.; Jayatilaka, D.; Spackman, M. A. *Chem. Commun.* **2007**, 3814–3816. (f) Spackman, M. A.; Jayatilaka, D. *CrystEngComm* **2009**, *11*, 19–32.

(33) d_{norm} represents a contact distance normalized to the van der Waals radii of the atoms. The use of this parameter has been found to be very useful to identify all close contacts even for complex crystal structures, see for examples:(a) Clark, T. E.; Makha, M.; Sobolev, A. N.; Raston, C. L. *Cryst. Growth Des.* **2008**, *8*, 890–896. (b) Aburaya, K.; Nakano, K.; Sada, K.; Yoswathananont, N.; Shigesato, M.; Hisaki, I.; Tohnai, N.; Miyata, M. *Cryst. Growth Des.* **2008**, *8*, 1013–1022.

(34) Wolff, S. K.; Grimwood, D. J.; McKinnon, J. J.; Jayatilaka, D.; Spackman, M. A. *CrystalExplorer2.1*; University of Western Australia: Crawley, Western Australia, 2007 (http://hirshfeldsurface.net/CrystalExplorer).

(35) Two exceptions are for CB[6] and CB[8] that can sometimes be isolated as crystals in which the macrocycles stack perfectly on top of each other in one dimension. See ref 12.

(36) *CrystalExplorer2.1* is a powerful software tool that enables an easy representation of intermolecular close contacts of molecules in crystals, using Hirshfeld surfaces, that represents the contact boundaries between closely packed molecules such that they never overlap. The volume obtained is highly dependent on the molecular geometry that was used to define the surface and also on the surrounding molecules. It thus enables one to gain considerable insights regarding the nature and the position of close contacts on that surface, that relate directly to the molecule under study.

(37) The purpose of the study in which a crystal structure of CB[7] was reported (ref 22) was to try to correlate the crystal structure (CB[7] assembly) with the gelation properties of the macrocycle. That in the seminal paper by Kim et al. was first reported as a definitive proof of the macrocyclic structure of CB[7] (ref 2c). Consequently, hydrogens were not located for all molecules in these structures. With this in mind, the data tentatively extracted from the literature crystal structure of CB[7] (ref 22) are not entirely accurate owing to the absence of hydrogen atoms on solvent and guest molecules (Hirshfeld surface analysis of CB[7]). Nonetheless, the reliable use of Hirshfeld surface analyses for crystals having disordered guest molecules has been reported, see for example:Makha, M.; McKinnon, J. J.; Sobolev, A. N.; Spackman, M. A.; Raston, C. L. *Chem.—Eur. J.* **2007**, *13*, 3907–3912.

(38) (a) Mammen, M.; Choi, S.-K.; Whitesides, G. M. *Angew. Chem., Int. Ed.* **1998**, *37*, 2754–2794. (b) Monsigny, M.; Mayer, R.; Roche, A. C. *Carbohydr. Lett.* **2000**, *4*, 35–52. (c) Kiessling, L. L.; Young, T.; Gruber, T. D.; Mortell, K. H. *Glycoscience* **2001**, *2*, 1817–1861. (d) Kitov, P. I.; Bundle, D. R. *Carbohydrate-Based Drug Discovery* **2003**, *2*, 541–574. (e) Mulder, A.; Huskens, J.; Reinhoudt, D. N. *Org. Biomol. Chem.* **2004**, *2*, 3409–3424. (f) Badjic, J. D.; Nelson, A.; Cantrill, S. J.; Turnbull, W. B.; Stoddart, J. F. *Acc. Chem. Res.* **2005**, *38*, 723–732. (g) An, Q.; Li, G.; Tao, C.; Li, Y.; Wu, Y.; Zhang, W. *Chem. Commun.* **2008**, 1989–1991. (h) Deyev, S. M.; Lebedenko, E. N. *BioEssays* **2008**, *30*, 904–918. (i) Sriram, S. M.; Banerjee, R.; Kane, R. S.; Kwon, Y. T. *Chem. Biol.* **2009**, *16*, 121–131.

(39) The d_e versus d_i diagram is a convenient 2D display to picture all close contacts surrounding the molecule under study. It represents for each situation when two atoms are sufficiently close in space, the distance between the Hirshfeld surface (positioned in between the two atoms), and the external atom (d_e) versus the distance between the Hirshfeld surface and the internal atom (d_i). All intermolecular interactions can thus be defined using a set of these two coordinates such that the closer the position is to the origin, the stronger the interaction.

(40) Pedzisa, L.; Hay, B. P. *J. Org. Chem.* **2009**, *74*, 2554–2560.

(41) Bondi, A. *J. Phys. Chem.* **1964**, *68*, 441–451.

(42) In the following example, Kögerler et coll. used this particular feature to grow cocrystals with electron-rich polyoxometalates:Fang, X.; Kögerler, P.; Isaacs, L.; Uchida, S.; Mizuno, N. *J. Am. Chem. Soc.* **2009**, *131*, 432–433.
(43) Desiraju, G. R. *Acc. Chem. Res.* **2002**, *35*, 565–573.
(44) Wang, Z.-G.; Zhou, B.-H.; Chen, Y.-F.; Yin, G.-D.; Li, Y.-T.; Wu, A.-X.; Isaacs, L. *J. Org. Chem.* **2006**, *71*, 4502–4508.
(45) Stancl, M.; Necas, M.; Taraba, J.; Sindelar, V. *J. Org. Chem.* **2008**, *73*, 4671–4675.
(46) Hexam, J. G.; Frey, M. H.; Opella, S. J. *J. Chem. Phys.* **1982**, *77*, 3847–3856.
(47) Bardelang, D.; Udachin, K. A.; Ripmeester, J. A.; Ratcliffe, C. I. To be published.
(48) Opella, S. J.; Frey, M. H. *J. Am. Chem. Soc.* **1979**, *101*, 5854–5856.
(49) In no instance was it possible to isolate CB[5] as a pure macrocycle after separation (addition of acetone to the last filtrate) during the purification process, precluding structural comparisons with **CB[5]C** and **CB[5]A** (directly obtained from the purification steps) by PXRD. In all cases we had to recrystallize it to obtain the pure material and this is another reason why we prepared **CB[5]A** from **CB[5]C**.
(50) The CB[8] solid filtered from the suspension obtained directly from the separation process (i.e., before recrystallization to give **CB-[8]C**) showed a PXRD pattern nearly identical to that of Figure 9h. This indicates that CB[8] has a strong tendency to structure itself according to crystal structure **4** since all three patterns from **CB[8]C**, **CB[8]A** and this CB[8]-as-prepared are very similar.
(51) (a) Dantz, D. A.; Meschke, C.; Buschmann, H.-J.; Schollmeyer, E. *Supramol. Chem.* **1998**, *9*, 79–83. (b) Kellersberger, K. A.; Anderson, J. D.; Ward, S. M.; Krakowiak, K. E.; Dearden, D. V. *J. Am. Chem. Soc.* **2001**, *123*, 11316–11317. (c) Miyahara, Y.; Abe, K.; Inazu, T. *Angew. Chem., Int. Ed.* **2002**, *41*, 3020–3023. (d) Grechin, A. G.; Buschmann, H.-J.; Schollmeyer, E. *Angew. Chem., Int. Ed.* **2007**, *46*, 6499–6501.
(52) Ultrasound can also promote crystallization in certain cases, see (a) Ruecroft, G.; Hipkiss, D.; Ly, T.; Maxted, N.; Cains, P. W. *Org. Process Res. Dev.* **2005**, *9*, 923–932and references therein. (b) Bucar, D.-K.; MacGillivray, L. R. *J. Am. Chem. Soc.* **2007**, *129*, 32–33. (c) Luque de Castro, M. D.; Priego-Capote, F. *Ultrason. Sonochem.* **2007**, *14*, 717–724. (d) Bardelang, D.; Camerel, F.; Margeson, J. C.; Leek, D. M.; Schmutz, M.; Zaman, Md. B.; Yu, K.; Soldatov, D. V.; Ziessel, R.; Ratcliffe, C. I.; Ripmeester, J. A. *J. Am. Chem. Soc.* **2008**, *130*, 3313–3315.
(53) (a) Terech, P.; Weiss, R. G. *Chem. Rev.* **1997**, *97*, 3133–3159. (b) Estroff, L. A.; Hamilton, A. D. *Chem. Rev.* **2004**, *104*, 1201–1217. (c) Sangeetha, N. M.; Maitra, U. *Chem. Soc. Rev.* **2005**, *34*, 821–836. (d) George, M.; Weiss, R. G. *Acc. Chem. Res.* **2006**, *39*, 489–497.
(54) (a) Ajayaghosh, A.; Praveen, V. K. *Acc. Chem. Res.* **2007**, *40*, 644–656. (b) Camerel, F.; Bonardi, L.; Schmutz, M.; Ziessel, R. *J. Am. Chem. Soc.* **2006**, *128*, 4548–4549. (c) Bardelang, D.; Camerel, F.; Ziessel, R.; Schmutz, M.; Hannon, M. J. *J. Mater. Chem.* **2008**, *18*, 489–494.
(55) Cations are usually observed to lid the CB cavities, see(a) Buschmann, H.-J.; Cleve, E.; Schollmeyer, E. *Inorg. Chim. Acta* **1992**, *193*, 93–97. (b) Jeon, Y.-M.; Kim, J.; Whang, D.; Kim, K. *J. Am. Chem. Soc.* **1996**, *118*, 9790–9791. (c) Whang, D.; Heo, J.; Park, J. H.; Kim, K. *Angew. Chem., Int. Ed.* **1998**, *37*, 78–80. (d) Buschmann, H.-J.; Jansen, K.; Meschke, C.; Schollmeyer, E. *J. Sol. Chem.* **1998**, *27*, 135–140. (e) Heo, J.; Kim, S.-Y.; Whang, D.; Kim, K. *Angew. Chem., Int. Ed.* **1999**, *38*, 641–643. (f) Heo, J.; Kim, J.; Whang, D.; Kim, K. *Inorg. Chim. Acta* **2000**, *297*, 307–312. (g) Samsonenko, D. G.; Sokolov, M. N.; Gerasko, O. A.; Virovets, A. V.; Lipkowski, J.; Fenske, D.; Fedin, V. P. *Russ. Chem. Bull., Int. Ed.* **2003**, *52*, 2132–2139. (h) Ong, W.; Kaifer, A. E. *J. Org. Chem.* **2004**, *69*, 1383–1385. (i) Zhang, F.; Yajima, T.; Li, Y.-Z.; Xu, G.-Z.; Chen, H.-L.; Liu, Q.-T.; Yamauchi, O. *Angew. Chem., Int. Ed.* **2005**, *44*, 3402–3407. (j) Samsonenko, D. G.; Gerasko, O. A.; Virovets, A. V.; Fedin, V. P. *Russ. Chem. Bull., Int. Ed.* **2005**, *54*, 1557–1562. (k) Liu, J.-X.; Long, L.-S.; Huang, R.-B.; Zheng, L.-S. *Cryst. Growth Des.* **2006**, *6*, 2611–2614. (l) Liu, J.-X.; Long, L.-S.; Huang, R.-B.; Zheng, L.-S. *Inorg. Chem.* **2007**, *46*, 10168–10173. (m) Zhang, Y.-Q.; Zhu, Q.-J.; Xue, S.-F.; Tao, Z. *Molecules* **2007**, *12*, 1325–1333. (n) Mezzina, E.; Cruciani, F.; Pedulli, G. F.; Lucarini, M. *Chem.—Eur. J.* **2007**, *13*, 7223–7233. (o) Feng, X.; Lu, X.-J.; Xue, S.-F.; Zhang, Y.-Q.; Tao, Z.; Zhu, Q.-J. *Inorg. Chem. Commun.* **2009**, *12*, 849–852. (p) Thuéry, P. *Inorg. Chem.* **2009**, *48*, 4497–4513.
(56) see for examples using cucurbiturils:(a) Mukhopadhyay, P.; Wu, A.; Isaacs, L. *J. Org. Chem.* **2004**, *69*, 6157–6164. (b) Liu, S.; Ruspic, C.; Mukhopadhyay, P.; Chakrabarti, S.; Zavalij, P. Y.; Isaacs, L. *J. Am. Chem. Soc.* **2005**, *127*, 15959–15967.
(57) (a) Tjivikua, T.; Ballester, P.; Rebek, J., Jr. *J. Am. Chem. Soc.* **1990**, *112*, 1249–1250. (b) Rowan, S. J.; Cantrill, S. J.; Cousins, G. R. L.; Sanders, J. K. M.; Stoddart, J. F. *Angew. Chem., Int. Ed.* **2002**, *41*, 898–952. (c) Corbett, P. T.; Leclaire, J.; Vial, L.; West, K. R.; Wietor, J.-L.; Sanders, J. K. M.; Otto, S. *Chem. Rev.* **2006**, *106*, 3652–3711. (d) Lehn, J.-M. *Chem. Soc. Rev.* **2007**, *36*, 151–160.
(58) (a) Mukhopadhyay, P.; Zavalij, P. Y.; Isaacs, L. *J. Am. Chem. Soc.* **2006**, *128*, 14093–14102. (b) Johnson, R. S.; Yamazaki, T.; Kovalenko, A.; Fenniri, H. *J. Am. Chem. Soc.* **2007**, *129*, 5735–5743. (c) Ludlow, R. F.; Otto, S. *Chem. Soc. Rev.* **2008**, *37*, 101–108. (d) Carnall, J. M. A.; Waudby, C. A.; Belenguer, A. M.; Stuart, M. C. A.; Peyralans, J. J.-P.; Otto, S. *Science* **2010**, *327*, 1502–1506.